Part II

DETAILED DISCUSSION

Part II DETAILED DISCUSSION

Chapter 1 Analysis of Existing Data

1.1 Organization to supply the existing data

The existing data has been collected from the Geological Information Center, Mineral Resources Authority of Mongolia (GIC, MRAM). The Geological Information Center stores all data on the geological surveys and mineral resources exploration conducted in Mongolia in the socialism period and the data on the geological surveys and mineral resources exploration conducted by Mongolia since the 1990 democratization. Only one set of the reports and related drawings is original. Although these documents can be freely accessed, it is not permitted to take out of the Geological Information Center. Also, a copy of the existing data on the Erdenet mine and its neighboring area was obtained from a Mongolian geologic engineer who had been working in the Erdenet Mining Corporation and Erdenet mine.

The literature was collected from GIC and through JICST (Japan Information Center of Science and Technology). The literature considered to be important was translated from Russian into English.

1.2 Types of the existing data

There are various types of obtained existing data, which are classified into the following categories. The details of the data are listed by classification (Appendix). The areas covered by the obtained data basically correspond to the Central north area of Mongolia.

-Literature (Appendix Table A-1)

-Deposit and mineral occurrence data (Appendix Table A-2)

A list (in Mongolian) of a total of 398 mineral occurrences within the area of this survey was translated into English.

- Topographical maps in 1:500,000 scale (6 sheets: Appendix Table A-3)

The topography is colored on the elevation contours. The national boundary and main roads and the name of main cities, towns, and villages, rivers, mountains, and lakes are described on the

maps in Mongolian.

- Topographical maps in 1:100,000 scale (48 sheets: Appendix Table A-3)
These black-and-white maps only show the neighborhood of the surveyed prospect. The evaluation, the name of main cities, towns, and villages, rivers, and mountains are described on the maps in Mongolian.

-Geology maps in 1:1,000,000 scale (2 sheets: Appendix Table A-4)

-Geology map in 1:500,000 scale (1 sheets: Appendix Table A-4)
This map was prepared jointly with the former Soviet Union in the 1900s.

- Mineral resource map in 1:500,000 scale (6 sheets including legends: Appendix Table A-4)

-Geology maps in 1:200,000 scale (20 areas: Appendix Table A-4, Figure A-1)
There are two types: the one (in Russian) was prepared jointly with the former Soviet Union before 1989 and the other (in Mongolian) was prepared by Mongolia alone after 1990. It has a supplementary report. The report consists of three chapters: Chapter 1: Geological structure, Chapter 2: Minerals and deposits, Chapter 3: Summary and future prospects. Only Chapter 3 was translated into English.

-Geology maps in 1:50,000 scale within the survey area (11 areas: Appendix Table A-4, Figure A-2)
The contents of these maps are the same as those of the above 1:200,000 scale geology maps. A supplementary report is also provided.

-Geology maps around the prospects (29 mineral occurrences: Appendix Table A-5)
Geology maps of the neighboring areas including the first year survey prospect.

-Mineral occurrences file (19 mineral occurrences)
The second year survey was conducted in the Tariat, Tosontsengel, Tsagaan uul, and Murun West areas. This file contains the mineral occurrences data, geology maps, and other documents prepared in English by the counterpart based on this survey.

-Geology maps and borehole log around the prospects (Appendix Table A-6)

Geology maps and past survey results (borehole log and others) of the prospects where the second year survey was conducted. The legends and descriptions were translated into English.

-Geological maps of Erdenet mine and its neighboring area, and drawings showing the geochemical and geophysical exploration results (Appendix Table A-7)
Various scales are used. The maps were drawn in monochrome and color. Plane view and cross section. The survey and preparation were mainly conducted in 1980s.

-Geophysical exploration within the survey area (Appendix Table A-8, Figure A-3)
Electrical exploration (Resistivity, IP), electromagnetic exploration, magnetic prospecting, airborne magnetic prospecting, and airborne gamma ray survey.

1.3 Analysis of the existing data

The description of the copper and gold prospects in the prospect and deposit lists was used to select a Grand Truth point. In particular, attention was paid to the grade (Standard: $\geqq$0.02% Cu, $\geqq$ 0.01 g/t Au) and the scale and description of alteration zones.

Data (geology maps and geochemical and geophysical exploration drawings) of the neighborhood of the Grand truth point was used during the site survey period to make the survey more efficient.

Chapter 2 Analysis of Satellite Images

2.1 Processing and production of SAR image

2.1.1 Introduction

(1) Purpose

Purpose was to produce digital mosaic images using JERS-1/SAR data for the central north area of Mongolia ranging from 48° to 52° N latitude and from 96° to 105° E longitude (excluding the area belonging to Russian Federation). Size of a unit of mosaic image was 1° in N-S by 1.5° E-W. The mosaic image of the whole area was also produced.

(2) Method

Method of processing and prosecution of image were described as follows:

① Bit conversion, trend correction, calculation of relative positions, conjunction of scenes and density adjustment were conducted on JERS-1/SAR data to prepare digital mosaic images.

②By comparing digital mosaic images with the topographic map, geographical coordinate systems were assigned to the images. Then, the images were cut out for each unit of sheet (1° in N-S by 1.5° in S-W).

③Individual sheet was stitched with each other to produce the mosaic image of the whole area.

(3) Outline of the area

The area is located in the central north area of Mongolia, ranging from 48° to 52° N latitude and from 96° to 105° E longitude (excluding the area belonging to Russian Federation), ranging approximately 250,000 km^2 (Figure II-2-1). The area corresponds to the west of Lake Baykal. While the southern part includes many steppes and swamps, the northern part consists of mountains of higher than 3,000 m above the sea level.

2.1.2 Satellite data

JERS-1/SAR data to cover the area consists of 141 scenes when each scene is expressed as a square. However, since some part of the 141 scenes belongs to Russia, the actual area inside Mongolia would be in a shape of a convex, that is its northwest and northeast corners lacking from

a whole square. Therefore, a total of 130 scenes were actually used to prepare the entire mosaic images (Table II-2-1 and Figure II-2-2).

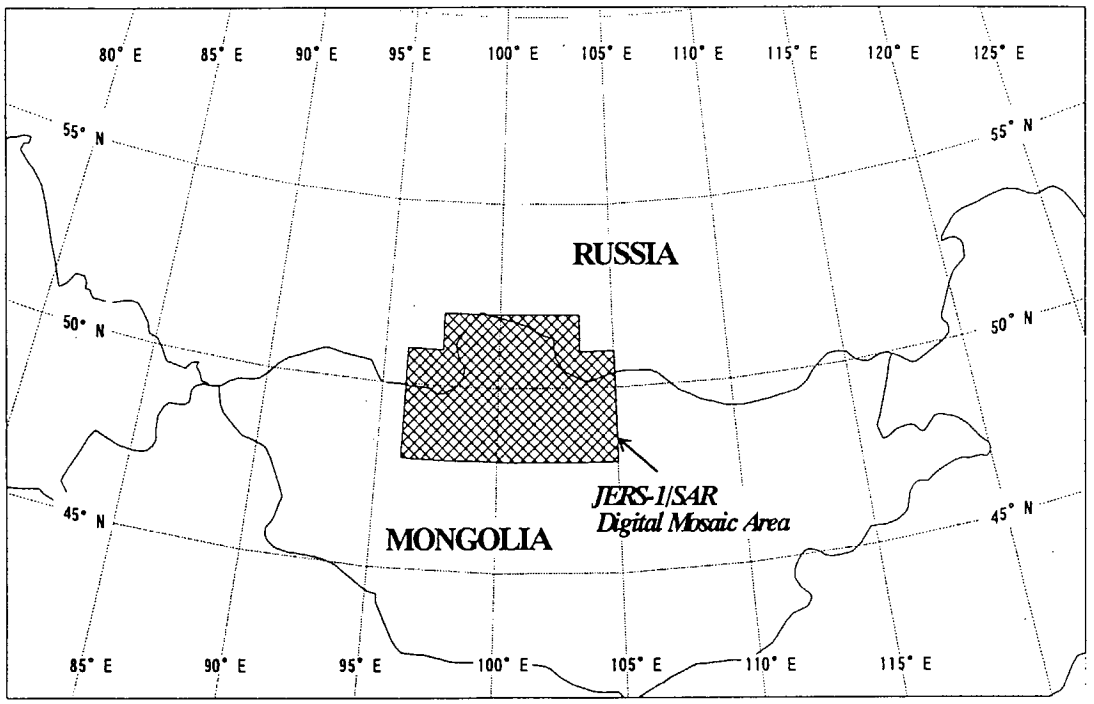

Fig. II-2-1 Location of satellite image analysis

Table II-2-1 List of JERS-1/SAR data

Path	Row	Date	N/U
135	218	1997/04/24	※
	219	1997/04/24	
	220	1997/04/25	
136	216	1997/04/25	
	217	1997/04/25	
	218	1997/04/25	
	219	1997/04/25	
	220	1997/04/26	
137	215	1997/04/26	
	216	1997/04/26	
	217	1997/04/26	
	218	1997/04/26	
	219	1997/04/26	
	220	1997/04/27	
138	213	1997/04/27	※
	214	1997/04/27	※
	215	1997/04/27	
	216	1997/04/27	
	217	1997/04/27	
	218	1997/04/27	
	219	1997/04/27	
	220	1995/07/08	
139	213	1994/01/26	※
	214	1995/07/08	
	215	1995/07/08	
	216	1995/07/08	
	217	1995/07/08	
	218	1995/07/08	
	219	1995/07/08	
	220	1997/04/29	
140	213	1997/04/29	
	214	1997/04/29	
	215	1997/04/29	
	216	1997/04/29	
	217	1997/04/29	
	218	1997/04/29	
	219	1997/04/29	
	220	1993/05/09	
141	213	1995/01/15	
	214	1993/05/09	
	215	1993/05/09	
	216	1993/05/09	
	217	1993/05/09	
	218	1993/05/09	
	219	1997/04/30	
	220	1997/05/01	

Path	Row	Date	N/U
142	213	1997/05/01	
	214	1997/05/01	
	215	1997/05/01	
	216	1997/05/01	
	217	1997/05/01	
	218	1997/05/01	
	219	1997/05/01	
	220	1997/05/02	
143	213	1997/05/02	
	214	1997/05/02	
	215	1997/05/02	
	216	1997/05/02	
	217	1997/05/02	
	218	1997/05/02	
	219	1997/05/02	
	220	1997/05/03	
144	213	1997/05/03	
	214	1997/05/03	
	215	1997/05/03	
	216	1997/05/03	
	217	1997/05/03	
	218	1997/05/03	
	219	1997/05/03	
	220	1997/05/04	
145	213	1994/02/01	
	214	1994/02/01	
	215	1994/02/01	
	216	1994/02/01	
	217	1994/02/01	
	218	1994/02/01	
	219	1994/02/01	
	220	1994/02/02	
146	213	1994/02/02	
	214	1994/02/02	
	215	1994/02/02	
	216	1994/02/02	
	217	1994/02/02	
	218	1994/02/02	
	219	1994/02/02	
	220	1994/02/02	
147	213	1997/05/06	
	214	1997/05/06	
	215	1997/05/06	
	216	1997/05/06	
	217	1997/05/06	
	218	1997/05/06	
	219	1997/05/06	
	220	1997/05/07	

Path	Row	Date	N/U
148	213	1997/05/07	
	214	1997/05/07	
	215	1997/05/07	
	216	1997/05/07	
	217	1997/05/07	
	218	1997/05/07	
	219	1997/05/07	
	220	1997/05/08	
149	213	1997/05/08	
	214	1997/05/08	
	215	1997/05/08	
	216	1997/05/08	
	217	1997/05/08	
	218	1997/05/08	
	219	1997/05/08	
	220	1997/05/09	
150	213	1997/05/09	
	214	1997/05/09	
	215	1997/05/09	
	216	1997/05/09	
	217	1997/05/09	
	218	1997/05/09	
	219	1997/05/09	
	220	1997/05/10	
151	213	1997/05/10	
	214	1997/05/10	
	215	1997/05/10	
	216	1997/05/10	
	217	1997/05/10	
	218	1997/05/10	
	219	1997/05/10	
	220	1997/05/11	
152	213	1997/05/11	※
	214	1997/05/11	※
	215	1997/05/11	
	216	1997/05/11	
	217	1997/05/11	
	218	1997/05/11	
	219	1997/05/11	
153	213	1997/05/12	※
	214	1997/05/12	※
	215	1997/05/12	
	216	1997/05/12	
	217	1997/05/12	
154	213	1997/05/13	※
	214	1997/05/13	※
	215	1997/05/13	※

Mark ※ in N/U column shows JERS-1/SAR data that is not used for production of the mosaic image

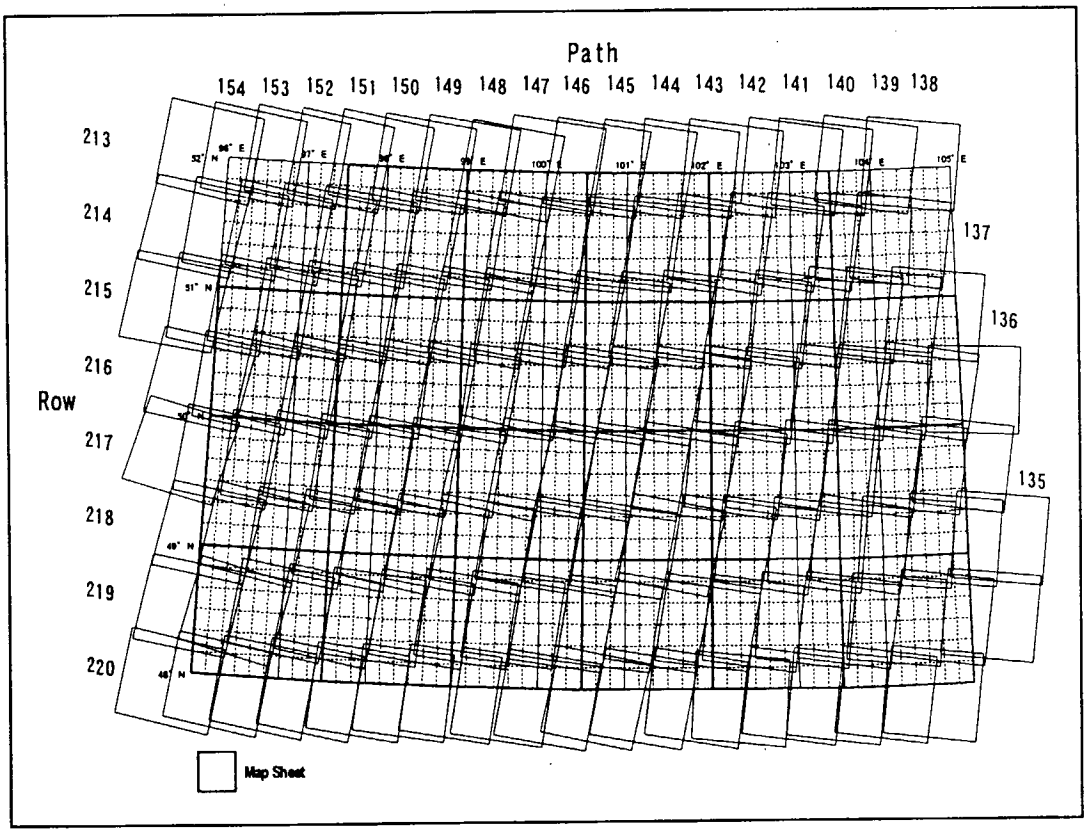

Fig. II-2-2 Index map of JERS-1/SAR data

2.1.3 Hardware and software

The following equipments to produce images were employed:

Hardware: HP9000 series J200 (OS: HP-UX 10.01)

Software : ERDAS Imagine (Ver 8.2) and in-house software for image processing.

2.1.4 Data processing

(1) Production of digital mosaics

Figure II-2-3 shows a flow of producing digital mosaic images. Mosaic wsd produced for a sheet of 1° in N-S by 1.5° in E-W. In order to acquire basic information of the data, a histogram of 16 bit data was output for all the data, and condition of the images was checked through visual inspection.

① Bit conversion

Since JERS-1/SAR level 2.1 data were provided in 16 bits with marks, the data were converted into 8 bit data after calculation of the basic statistic quantity. Since 16 bit data themselves represented their physical quantities, if individual scenes were converted into 8 bits in different width, relative relation of physical quantities within their original data would be damaged. This would appear in difference in gray level among images when they are stitched. Therefore it is better to stretch all the data in the same width in converting them into 8 bits. When conducting bit conversion, taking into consideration that the form of histogram of the data in 16 bits is unsymmetry, we compared typical histogram representing areas from swamps to mountains with each other. Then the stretching width was determined to be the range in which image characteristics of the original data remains as much as possible over these areas. The stretch width used was from 0 to 2800.

②Trend correction

In JERS-1/SAR image there is a trend which is in parallel with the azimuth direction (direction of the satellite orbit) and changes toward direction of the range (direction of radar irradiation). The trend was extracted from the image, and after obtaining difference between average of all the data and the trend, the difference was subtracted from the original image. When extracting the trend, image data which is not occupied by many lakes and mountains, that is parts with little

variation, were employed. If it is impossible to extract trend from the image, trend extracted from another image is used for correction of the image.

③ Calculation of relative positions

To produce satellite image mosaics in general, Ground Control Point (GCP) was established for each scene, and geographical coordinate systems were assigned to them before they were stitched. However, in case that it is difficult to decide GCP because topographic map of the relevant area is not accurate or surface characteristics is lacking, the effect is focusing on a part of its mosaic image resulting in distortion and accuracy in its conjunction is excessively degraded. In some cases due to deflection of the satellite orbit, positional shift happens between JERS-1/SAR images which are projected onto the UTM coordinate. Therefore, we applied a method of calculating relative positions among images as rotational component, and by rotating the images to avoid their possible positional changes. Here, positions were adjusted through mutual rotation of images whose process is shown in Figure II-2-4 so that possible changes might not be focused on a certain point.

First, image data of four scenes adjacent to one another were handled in a suite and their mutual rotating angles α_{AB}, α_{BC}, α_{CD} and α_{DA} were obtained. Then, 1/4 of θ, the final difference in angles arising from the rotation of the images was assigned to the four scenes, and individual image data were rotated in accordance with the resulting angles. In consequence, 1/4 of θ, the difference in angles obtained through assignment to the four scenes becomes an error arising from stitches of the four scenes.

④ Conjunction of scenes and adjustment of gray level

The image data rotated by calculating their relative positions were conjugated in accordance with the relative positions obtained. Because there is difference in gray levels because of time gap of the data acquisition, the images were conjugated after adjusting the gray levels. For adjustment of gray levels, the statistics of levels were determined on the portion where the conjugated scenes overlapped, and average value and standard deviation of each scene was modified to be consistent.

(2) Geometric correction of mosaics

In order to allocate geographical coordinate to the produced mosaics, geometric correction was conducted by comparing TM images with the topographic map data. Since topography of this area in scale of 1:500,000 of Tactical Pilotage Chart (TPC) was digitized, GCPs were determined based on these data and then geometric correction was done. The GCPs were 10 to 12 in number per one sheet of the image. We set as many GCPs as possible to be located in the periphery of a sheet of the image, and a few inside the image, and tried GCPs to keep uniform distance with each other.

For geometric correction, the third affine transformation was used to decrease the total RMS errors to be less than ten. In order that the statistics of the original data is not demolished, resampling was conducted using the nearest method, and the final pixel size was decided to be12.5 m, the same as that of the original data.

The coordinate used was the UTM (Universal Transverse Melcatol) projection and "Krasovsky" was used for ellipsoid. In the UTM projection, a zone is set up with the width of three degrees of longitude in E-W direction from central meridian. Since 102° E longitude was a boundary between Zone 47 and Zone 48 in this area, 15 images located in the west of 102° E longitude were determined to be in Zone 47, and 7 images located to the east from there were determined to be in Zone 48.

(3) Cutting out and filtering

The mosaics to which the UTM coordinate were allocated were cut out in 1° in N - S by 1.5° in E-W. In the trimming, an overlapped portion of 5′ each was left from the northwest corner to the northern and western directions, and from the southeast corner to the eastern and southern directions. When outputting images, a median filter of 3 pixels by 3 pixels was used to prevent roughness of the surface affected by speckle noise peculiar to SAR data so that detailed information might be visible. A print of 1:200,000 scale was output with titles and scales indicated.

Name given to an individual image was derived from major municipalities or lakes located in the area of the image. Table II-2-2 and Figure II-2-5 show a list of individual images and index map respectively, and Figure II-2-6 shows an example of the output of the image.

(4) Preparation of mosaic image of the entire area

In addition to the images of 1° (N-S) by 1.5° (E-W), the mosaic image of the entire area was also produced. The coordinate was already allocated to each image. However, since the images extended over two zones of the UTM coordinate, it was necessary to unify the coordinate system in preparing the mosaic image of the entire area. It was possible to unify them to either of the two

UTM zones. However, in areas of high latitudes like this area, the more they are away from the central meridian, the more distorted the coordinate would be. Therefore, Lambert's conformal projection method was applied which is suitable to project areas of medium latitudes. A print 1:1,000,000 scale was output with titles and scales indicated, etc. Figure II-2-7 shows the mosaic image of the entire area.

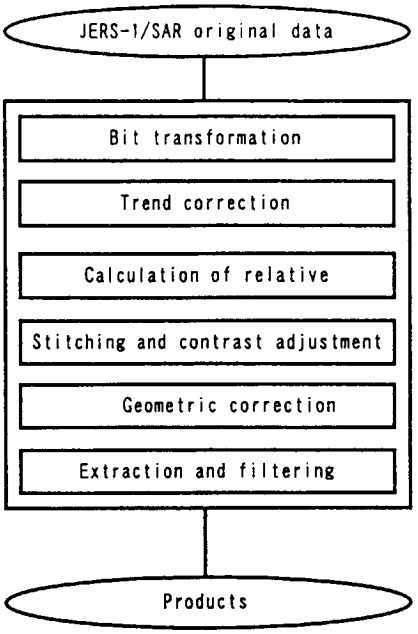

Fig. II-2-3 Flow chart of producing JERS-1/SAR mosaic image

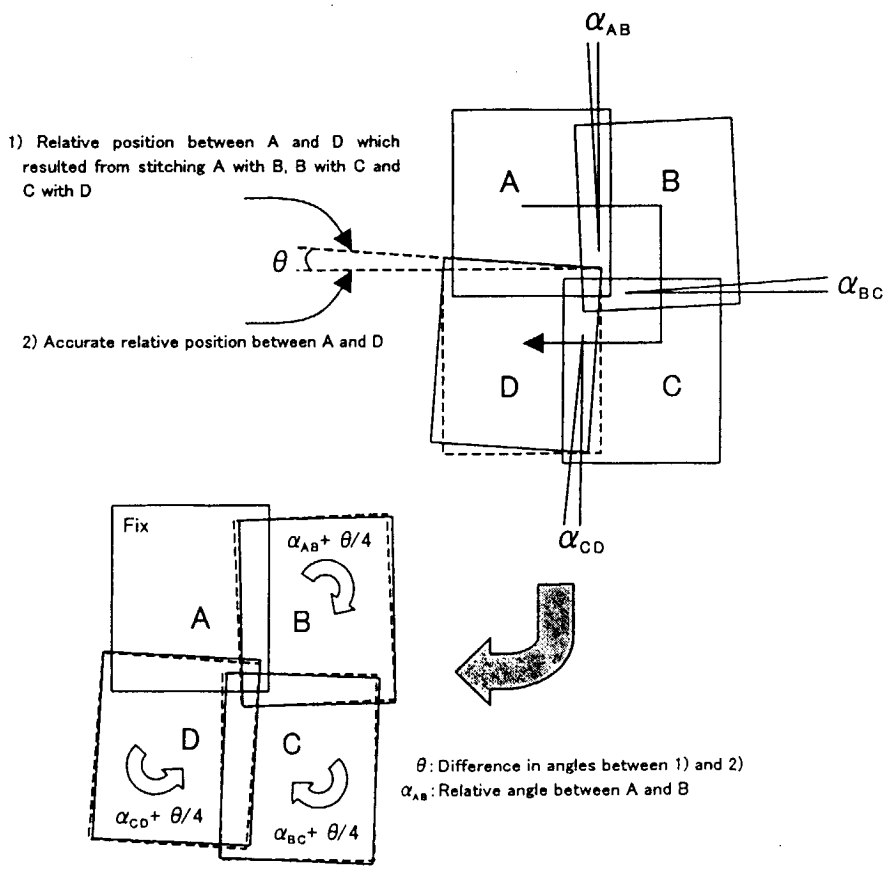

Fig. II-2-4 Process of stitching 4 scenes of JERS-1/SAR data

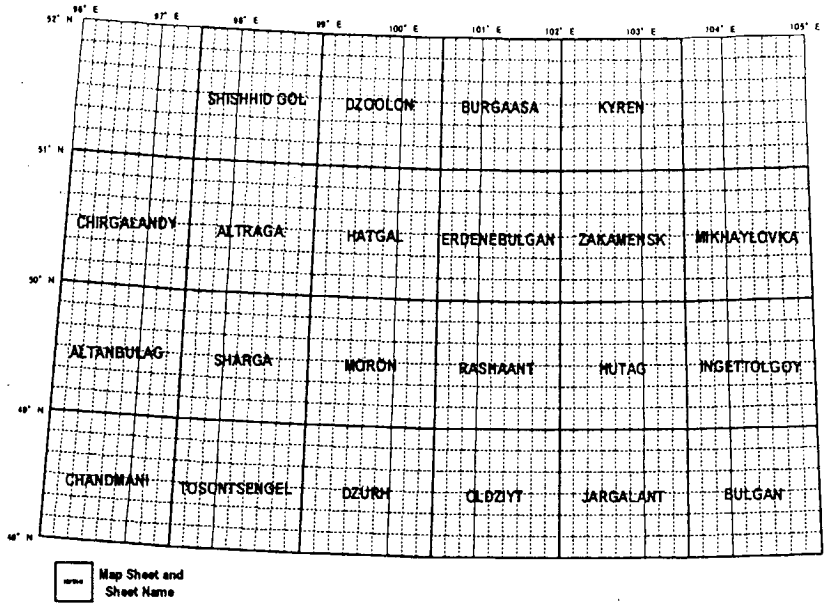

Fig. II-2-5 Index map of JERS-1/SAR mosaic images

Table II-2-2 List of JERS-1/SAR mosaic images

Image Unit	*Corner of the left upper side*		*Corner of the right upper side*		*UTM Zone*
	Longitude	*Latitude*	*Longitude*	*Latitude*	
SHISHHID GOL	N97°30'	E52°00'	N99°00'	E51°00'	N47
DZÖÖLÖN	N99°00'	E52°00'	N100°30'	E51°00'	N47
BURGAASA	N100°30'	E52°00'	N102°00'	E51°00'	N47
KYREN	N102°00'	E52°00'	N103°30'	E51°00'	N48
CHIRGALANDY	N96°00'	E51°00'	N97°30'	E50°00'	N47
ALTRAGA	N97°30'	E51°00'	N99°00'	E50°00'	N47
HATGAL	N99°00'	E51°00'	N100°30'	E50°00'	N47
ERDENEBULGAN	N100°30'	E51°00'	N102°00'	E50°00'	N47
ZAKAMENSK	N102°00'	E51°00'	N103°30'	E50°00'	N48
MIKHAYLOVKA	N103°30'	E51°00'	N105°00'	E50°00'	N48
ALTANBULAG	N96°00'	E50°00'	N97°30'	E49°00'	N47
SHARGA	N97°30'	E50°00'	N99°00'	E49°00'	N47
MÖRÖN	N99°00'	E50°00'	N100°30'	E49°00'	N47
RASHAANT	N100°30'	E50°00'	N102°00'	E49°00'	N47
HUTAG	N102°00'	E50°00'	N103°30'	E49°00'	N48
INGETTOLGOY	N103°30'	E50°00'	N105°00'	E49°00'	N48
CHANDMANI	N96°00'	E49°00'	N97°30'	E48°00'	N47
TOSONTSENGEL	N97°30'	E49°00'	N99°00'	E48°00'	N47
DAÜRH	N99°00'	E49°00'	N100°30'	E48°00'	N47
ÖLDZIYT	N100°30'	E49°00'	N102°00'	E48°00'	N47
JARGALANT	N102°00'	E49°00'	N103°30'	E48°00'	N48
BULGAN	N103°30'	E49°00'	N105°00'	E48°00'	N48

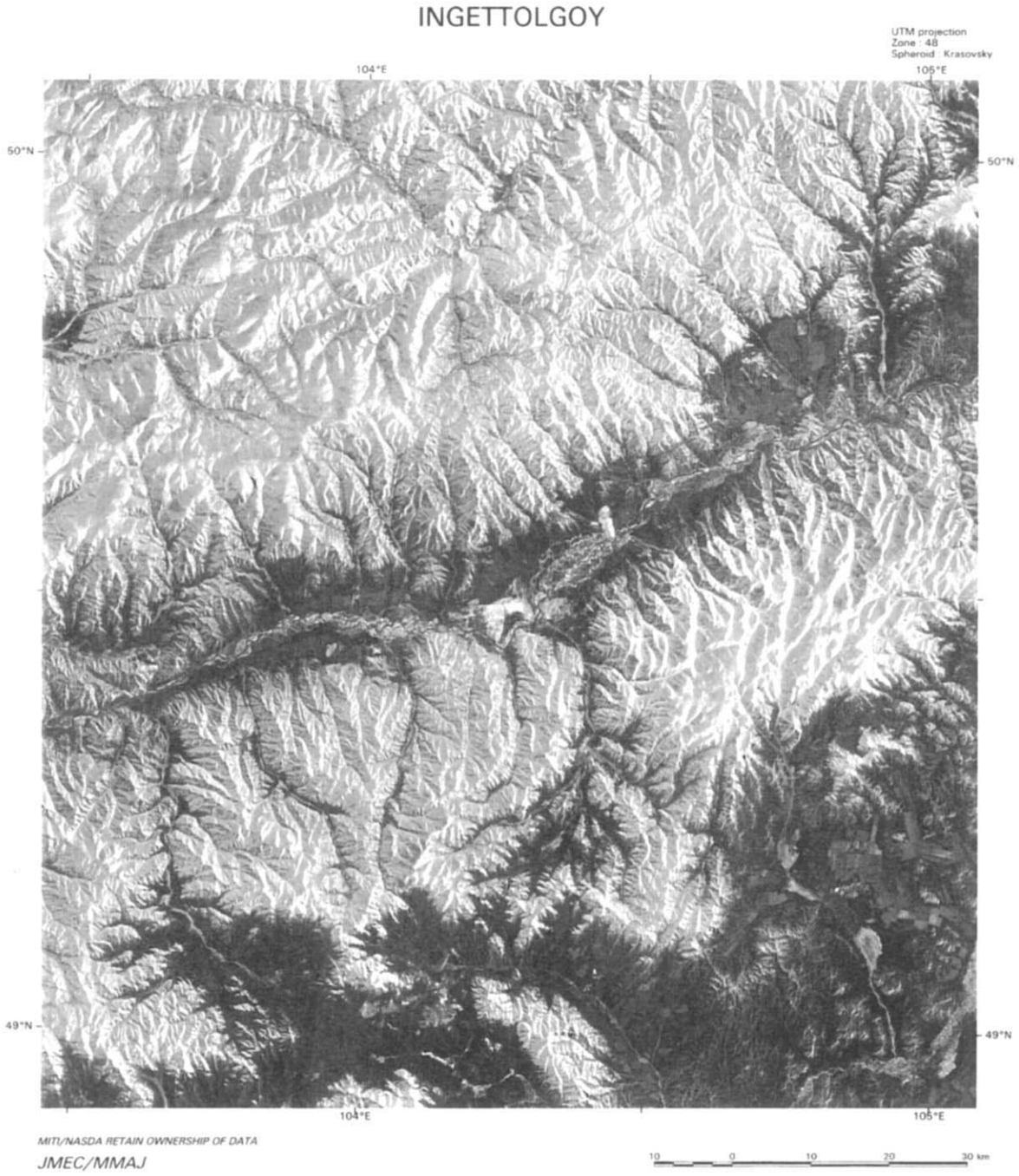

Fig. II-2-6 Example of 1:200,000 JERS-1/SAR mosaic image

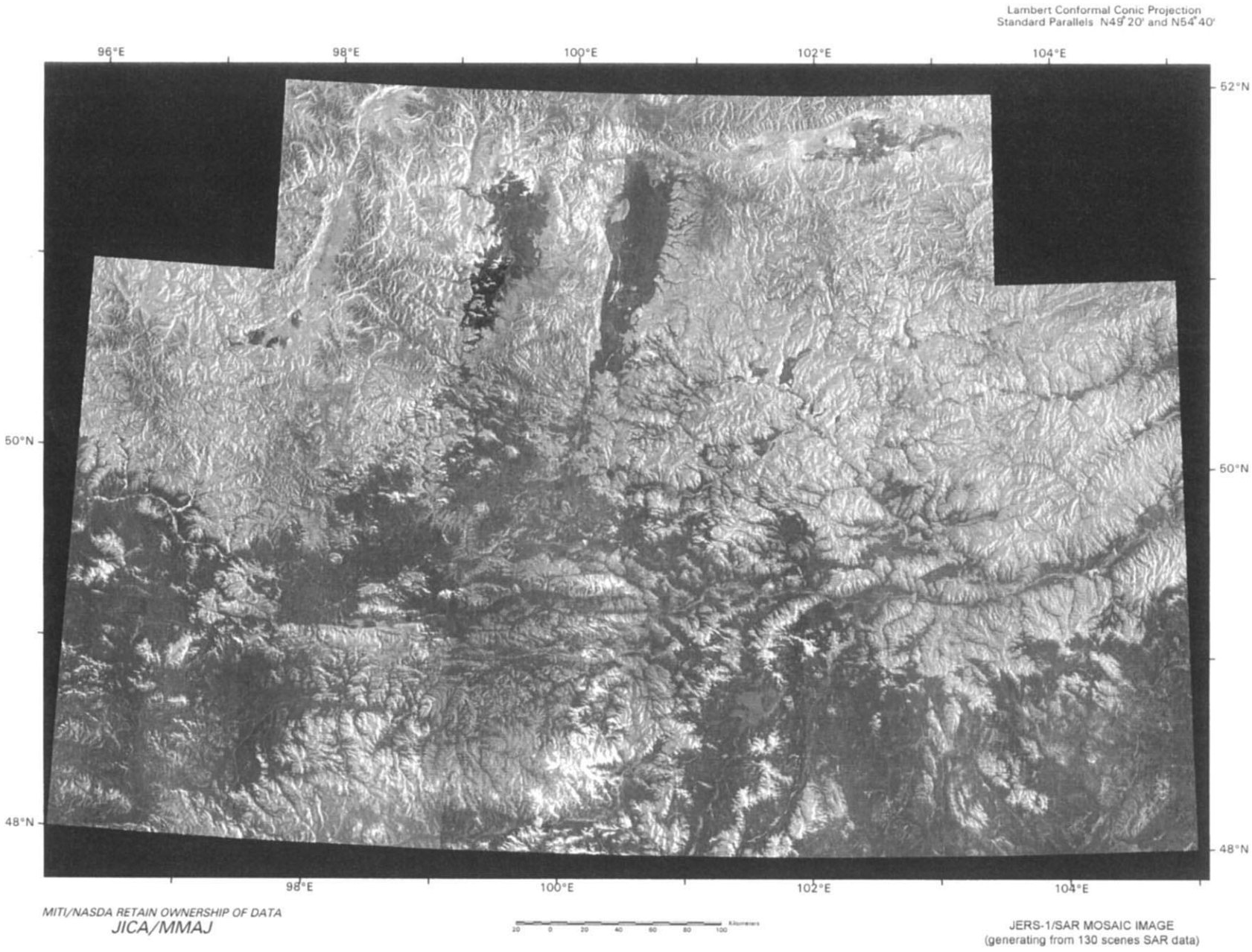

Fig. II-2-7 JERS-1/SAR mosaic image of the central north area

2.2 Analysis of the SAR image and its interpretation

2.2.1 Outline

The area covered for analysis of LANDSAT TM image was located in the northern central part of Mongolia ranging from 48° to 52° N latitude and from 100° 30′ to 105° E Longitude, within the border with Russian Federation in the northern end. The area is situated to the west of the capital Ulaanbaatar including Khuvsgul, Bulgan, and Arkhangay Provinces (Aimags). The northern part of the area is extremely steep with Khuvsgul Mountains, that is 2,200 to 3,351 m above the sea level, while the southern part mostly consists of smooth hills where vast steppe develops.

Conifers called "taiga" vegetate widely in the area where it is chilly and covered with snow and ice for a long period in winter. Since the image analysis covers a large entire area and it is difficult to obtain effective data through optical sensors under such a climatic environment, we employed a SAR (Synthetic Aperture Radar) of JERS-1.

Eleven digital mosaic images were used for the analysis, each of which covers 1° (N-S) by 1.5° (E-W) with the reduced scale of 1:200,000. Last year (in the initial year), eleven digital mosaic images were analyzed on the eastern half of the target area. In the survey conducted in this fiscal year, another eleven images were analyzed on the western half of the target area.

2.2.2 Method of analysis and interpretation

Division of geological unit and interpretation of geological structure including lineaments were conducted for the analysis. For division of geological unit, criteria described below were established to interpret photogeological features of the radar image. Then characteristic features were divided into some types in terms of each criterion, and geological unit was assigned to each of the types.

(1) Photographic features

- Color tones : dark, dark gray, gray and light gray
- Texture : coarse, intermediate and smooth

(2) Topographical features

- Drainage pattern: dendritic, parallel, semi-dendritic, semi-parallel and linear
- Drainage density: high, intermediate, low and extremely low
- Resistance: high, intermediate, low and extremely low
- Shape of ridge: sharp, round and flat
- Development of beddings: Clear, unclear and massive
-

2.2.3 Results of analysis and interpretation

(1) Division into geological units

In dividing the area into geological units based on the results of interpretation, we compared our interpretation results with the existing geological division referring to the existing geological maps of 1:500,000 scale, and decided names of geological units in accordance with symbols of the strata and rocks used in the geological map. Photographic and topographic features of individual geological units are shown in Table II-2-3.

Division of geological unit was determined mainly on the basis of topographical features. Since a variety of vegetation is involved in the area such as coniferous forests, steppes, swamps, naked land, etc., photographic features shown in the radar images are almost attributable to difference in densities of vegetation (trees in particular). In other words, as radar waves scatter much on the land where trees grow closely together, the land is shown in bright tones on the image. On the other hand, since radar waves scatter little on steppes and naked land, the land is shown in dark tones on the image.

Resistance and drainage density to which we attached the greatest importance in the interpretation are described as follows:

① Resistance

Resistance means a degree of resistance of strata and rocks against erosion.

The geological units with high resistance formed a high land, because it shows high coefficient of permeability of strata and rocks due to high porosity and developed fractures into which infiltration of rainwater is large and small quantity of rain flow on the land surface. Therefore, the degree of erosion is low. However, in the geological units with low resistance, much rain flows on the land surface because of low coefficient of permeability. This causes excessive erosion, and a low land is formed.

Table II-2-3a Characteristics of photogeologic units (sedimentary and volcanic rocks)

(1)

Unit	Photo-characteristics		Morphologic Expression					Comparison with existing map	
	Tone	Texture	Drainage Pattern	Drainage Density	Rock Resistance	Ridge Type	Bedding	Geologic Unit	Geologic Age and Main Lithology
Q5	dark to medium grey	rough	colinear	very low	very low	flat	none	Q, βQ	Quaternary: sand,gravel,clay basalt
Q4	dark to light grey	smooth	meandering, anastomotic sub-dendritic	low	very low	flat	none	QIV, (QIII-IV)	Quaternary: sand,gravel,clay
Q3	dark	smooth	colinear	very low	very low to low	flat	none	QIII-IV, QIII	Quaternary: sand,gravel,clay
Q2	dark	smooth	colinear	very low	very low to low	flat	none	QII-III	Quaternary: sand,gravel,clay
N1	dark grey to medium grey	medium to rough	sub-dendritic	low	moderate	flat	(lava flow band)	βN1, βN2	Quaternary(Pliocene): trachy-basalt,basalt
K1	dark grey to medium grey	smooth	sub-dendritic, sub-parallel	medium	low	sharp(wide)	unclear	K1	Cretaceous: conglomerate, sandstone,mudstone
J3-K1	dark to medium grey	smooth	sub-parallel	low	low	sharp(tight)	rare	J3-K1	Jurassic to Cretaceous: conglo-merate,sandsone
J1-2	medium grey to dark grey	smooth	sub-parallel	low	low	round	unclear	J1-2, J1-2sh	Jurassic: conglomerate,sand-stone,mudstone
T3-J1	dark grey to medium grey	medium	sub-dendritic	medium	low to moderate	sharp(wide)	partly bedded	T3-J1mg	Triassic to Jurassic: andesite basalt,tuff
T2-3	dark grey to medium grey	medium	sub-parallel	medium	moderate to high	sharp(wide)	unclear	T2-3, T2-3ab1～4	Triassic: sandstone,conglo-merate,siltstone
P2-T1	medium grey to light grey	rough	sub-dendritic	low to medium	high	subround to sharp(tight)	unclear	P2-T1hr3	Permian to Triassic: trachy-basalt,trachyandesite
P2v	dark grey to medium grey	medium to rough	dendritic	high	low to moderate	sharp(tight)	massive	P2hr4	Permian: trachybasalt, trachyandesite
P2	medium grey	medium	sub-parallel	medium	high	round	unclear	P2	Permian: conglomerate,sand-stone,siltstone
P1v(h)	dark to medium grey	rough	dendritic	high to medium	moderate to high	sharp(tight)	massive	P1-2hn2+3, P1hn2, P1hn1, P1-2hn3	Permian: rhyolite,dacite,ande-site,basalt,tuff,sandstone
P1v(l)	dark to medium grey	rough	dendritic	high to medium	low	sharp(tight)	massive	P1-2hn2+3, P1hn2, P1hn1, P1-2hn3	Permian: rhyolite,dacite,ande-site,basalt,tuff,sandstone

Table II-2-3a Characteristics of photogeologic units (sedimentary and volcanic rocks)

(2)

Unit	Photo-characteristics		Morphologic Expression					Comparison with existing map	
	Tone	Texture	Drainage Pattern	Drainage Density	Rock Resistance	Ridge Type	Bedding	Geologic Unit	Geologic Age and Main Lithology
C2	medium grey	medium	sub-dendritic, sub-parallel	medium	high	sharp(wide)	partly bedded	C2ar	Carboniferous: sandstone, conglomerate
C1	medium grey	smooth	sub-dendritic	low	high	round	unclear	C1	Carboniferous: conglomerate, sandstone,siltstone
C1ur	dark to medium grey	medium	sub-dendritic	low to medium	low to moderate	sharp(wide) to round	partly bedded	C1ur1, C1ur2	Carboniferous: siltstone,conglomerate,sandsote
D	medium grey	rough	sub-dendritic, sub-parallel	low to medium	high	subround to sharp(wide)	unclear	D	Devonian: conglomerate,sandstone,tuff,siltstone
D1-2	medium grey	smooth	sub-dendritic	low	high	round	unclear	D1-2	Devonian: siltstone,sandstone conglomerate
S-D1	medium grey	rough	sub-dendritic	medium	moderate	sharp(wide)	unclear	S-D1, S-D1hr	Silurian to Devonian: andesite dacite,rhyolite,tuff
€3-O	medium grey	rough	dedritic	low to medium	high	round	unclear	€3-O	Cambrian to Ordovisian: shale siltstone,phyllite,sandstone
€2-O1(h)	medium grey	medium	sub-dendritic	high	moderate to high	sharp(tight)	unclear	€2-O1	Cambrian to Ordovisian: sandstone,siltstone,phyllite,shale
€2-O1(l)	medium grey	medium	sub-dendritic, sub-parallel	very high	low	sharp(tight)	unclear	€2-O1	Cambrian to Ordovisian: sandstone,siltstone,phyllite,shale
€1	medium grey to light grey	rough	sub-dendritic	high	moderate to high	subround to sharp(wide)	unclear	€1,€1br, V- €1hs, V- €1, V- €1eg	Cambrian: limestone,dolomite
R3	medium grey	rough	sub-dendritic	medium	high	subround to sharp(wide)	partly bedded	R3, R3-V	Proterozoic: dolomite,quartzite limestone
R2	medium grey	rough	sub-dendritic	low to medium	high	subround to sharp(tight)	partly bedded	R2	Proterozoic: metaeffusive rocks metatuff,metasandstone
PR1	medium grey to light grey	rough	sub-dendritic	medium	high	sharp(wide)	unclear	PR1	Proterozoic: shale,amphibolite marble
AR2-PR1	medium grey to light grey	rough	sub-dendritic	low	high	sharp(wide) to round	unclear	AR2-PR1	Proterozoic: gneiss,amphibolite marble

Table II-2-3b Characteristics of photogeologic units (intrusive rocks)

(1)

Unit	Photo-characteristics		Morphologic Expression					Comparison with existing map	
	Tone	Texture	Drainage Pattern	Drainage Density	Rock Resistance	Ridge Type	Bedding	Geologic unit	Geologic Age and Main Lithology
γJ	medium grey to dark grey	rough	sub-parallel	high	moderate	sharp(tight)	none	γJ	Jurassic: granite,granite porpyry,diorite,granodiorite
γT3-J1	medium grey to dark grey	medium	sub-dendritic	low	moderate	sharp(wide)	none	γT3-J1	Triassic to Jurassic: granite, granodiorite
πγP2-T1	medium grey to dark grey	medium	sub-dendritic	low	low	round	none	πγP2-T1	Permian to Triassic: granite porphyry,plagioporphyry
γP2-T1	medium grey to light grey	rough	sub-dendritic	high	high	sharp(wide)	none	γP2-T1, γεP2-T1	Permian to Triassic: granite, granodiorite,gabbro
γP2	medium grey	rough	sub-dendritic	high	moderate to high	sharp(tight)	none	γP2	Permian: monzonite,syenite monzosyenite,granodiorite
εγP	light grey	rough	sub-dendritic	medium	high	subround	none	εγP	Permian: alkaline granite, syenite,granosyenite
γP	dark to medium grey	medium	sub-dendritic, sub-parallel	medium	low to high	round	none	γP	Permian: granite,granodiorite
γδC2-3	medium grey	rough to smooth	sub-dendritic	medium	high to moderate	sharp(tight) to sharp(wide)	none	γδC2-3, γC2-3	Carboniferous: granite,granodiorite,diorite,gabbro
εPZ2	medium grey	rough	sub-parallel	high	high	sharp(tight)	none	εPZ2	Middle Paleozoic: syenite, nordmarkite,palascite
γD2	medium grey	medium	sub-dendritic	medium	moderate to high	subround to sharp(tight)	none	γD2	Devonian: granite,granosyenite
γδS	medium grey	rough	sub-dendritic	medium	high	sharp(wide)	none	γδS	Silurian: granodiorite
γS	dark	smooth	sub-parallel	low	low	sharp(tight)	none	γS	Silurian: granite,adamellite
γ-γδPZ1	light gry to dark grey	rough to medium	sub-dendritic	medium	high to low	sharp(tight)	none	γ-γδPZ1	Early Paleozoic: granite, granodiorite,diorite
γPZ1	medium grey to light grey	rough	dendritic	medium	high	sharp(tight)	none	γPZ1	Early Paleozoic: biotite granite, plagiogranite

Table II-2-3b Characteristics of photogeologic units (intrusive rocks)

(2)

Unit	Photo-characteristics		Morphologic Expression					Comparison with existing map	
	Tone	Texture	Drainage		Rock Resistance	Ridge Type	Bedding	Geologic unit	Geologic Age and Main Lithology
			Pattern	Density					
γδPZ1	light grey	medium	sub-dendritic	medium	high	round to subround	none	γδPZ1	Early Paleozoic: adamellite, granodiorite,tonalite
νδPZ1	medium grey	rough	sub-dendritic	medium	moderate to high	sharp(tight) to subround	none	νδPZ1	Early Paleozoic: gabbro, gabbroic diorite,diorite
σR3-Є1	medium grey	rough	sub-parallel	medium	high	round	none	σR3-Є1	Riphean to Cambrian: dunite, harzburgite,wehrlite
γR	light grey to dark	rough	sub-dendritic	medium	high	subround	none	γR	Riphean: leucocratic granite, gneissose granite
νδPR	light grey to dark	medium	sub-dendritic	low	high	subround	none	νδPR	Proterozoic: anorthosite, gabbroic anorthosite
γPR1	medium grey	medium	sub-dendritic	low to medium	high	sharp(tight)	(schistose)	γPR1	Proterozoic: granitic gneiss, migmatite,granite

Typical examples of the rocks with high resistance are coarse sandstone, conglomerates, limestone and granites with few fractures. Typical rocks of the units in this area are acidic volcanic rocks of the Permian (Plv (h)), conglomerate (P2), sedimentary rocks of the Carboniferous (C1, C2), sedimentary rocks of the Devonian (D, D1-2, D2), sedimentary rocks of the Cambrian (Clhs), metamorphic rocks of the Proterozoic (R2, R3, PR1, AR2-PR1), granites of the early Paleozoic (γ PZ1) and granitic gneisses (γ PR1).

On the other hand, typical rocks with low resistance are mudstone, fine grain tuff, sedimentary rocks, etc., while typical rocks of the units in this area are unconsolidated sediments and basalt lava of the Quaternary (Q2-Q5, N1) and sedimentary rocks (J1-2, J3-K1, K1) of the Jurassic to the Cretaceous.

② Drainage density

Like resistance described to above, drainage density also has a close relation with quantity of rainwater flowing on the land surface. The more rain flows on the land surface, the more drainage are developed, and in case smaller amounts of rain flow on the land surface, drainage density becomes lower. In general, therefore, while the geological units with high drainage density tend to have low resistance, those with low drainage density tend to have high resistance. However, as an exceptional case, in unconsolidated and loose strata like sedimentary rocks of the Quaternary, both drainage density and resistance are low.

Rocks existing in geological units with high drainage density are basalts of the Permian (P2v), sedimentary rocks of the Cambrian to Ordovician (C2-01(h), C2-01(1)) and granites of the Permian to Ordovician (γ P2, γ P2-T1), etc.

On the other hand, rocks existing in geological units with low drainage density are unconsolidated sediments and basalt lava of the Quaternary (Q2-Q5, N1), sedimentary rocks of the Jurassic (J1-2), metamorphic rocks of the Proterozoic (AR2-PR1), granitic gneisses of the Proterozoic (γ PR1), etc.

(2) Analysis and interpretation of geological structures

During interpretation and analysis of geological structures, we extracted lineaments and circular structures. Out of the lineaments extracted, those which can be identified on the image as faults and those drawn as faults in the existing geological maps were determined to be faults and shown in the interpretation map.

① Fault and lineament

a. Eastern half of the target area

There is a difference between lineaments extracted from the valley of the Selenge river which flows to the east in the center and those extracted from the districts to the north and south of the valley.

In the central part, distinctive E-W lineaments which continues well were dominant, and short NW-SE lineaments were additionally noted. In the northern part of the valley where extraction density was low, short lineaments of the NW-SE and E-W trends were identified. In the southern part of the valley, lineaments of the NW-SE and N-S trends were dominant, and extraction density was high especially in the southeastern part.

In every place described above, lineaments of the NW-SE trend were identified. These lineaments intensively occur in the images ranging from the Bulgan 1:200,000 Sheet area which is located in the southeastern part of the survey area, through the southern part of Lake Khuvsgul situated in the northeastern part of the area, to the south of the lake in a width of approximately 200 km, diagonally crossing the E-W lineament in the central part.

b. Western half of the target area

A fracture in the E-W direction is developed westward from the Selenge river which flows eastward in the central part. The state of fracture development differs between its southern and northern parts.

In the "Duzurh" image of the southern part, fractures mainly in the NW-SE and NE-SW directions are developed. In the southern part of the area, a lineament in the E-W direction is also developed. This tendency continues westward up to the "Tosontsengel" image. However, in the east of the "Chandmani", a fracture in the NW-SE direction becomes dominant. In its west, the density of the lineament is extremely lowered.

The "Murun" image has a characteristic of having a high-density fracture in the E-W direction, and its density is lowered toward its northern part. This fracture in the E-W direction is continues toward the "Sharga" image in the west direction, and lineament density reduction is identified in its central part. Also in its northwestern part, a fracture in the NW-SE direction with its short extension is developed with high density. This tendency is continued up to the "Altanbulag" in its west.

The "Hatgal" image is located to the north of a fracture in the E-W direction. In addition to the fractures in the NW-SE and NE-SW directions, a fracture in the N-S direction is developed to meet the direction of the Khuvsgul Lake extension. The same tendency is noted in the "Altraga"

image to its west.

In the "Dzoolon" image, fractures in the NW-SE, NE-SW, N-S and E-W directions are developed along the northern border from the west bank of Lake Khuvsgul. In the central part of the area where sediments of the Quaternary are distributed, their densities are extremely lowered. In the "Shishhid Go"l image, the fractures in the same directions are distributed in medium-grade densities.

②Circular structure

a. Eastern half of the target area

The following circular structures below were identified in the area. It was interesting that circular structures extracted from the western part of the Jarganant sheet area and the southeastern part of the Hutag sheet area might have been formed by intrusion of small-scaled rocks and have accompanied alteration zones.

[Central part of the Erdenebulgan sheet area]

A circular structure having a diameter of 2 km was extracted from an area where granitic rocks of the early Proterozoic (γ δ PZ1) occur.

[Northern part of the Rashaant sheet area]

A circular structure having a diameter of 4 km was extracted from an area where a stratum of the Cambrian (C1) occur.

[Northern part of the Ingettolgoy sheet area]

A semi-circular structure having a diameter of 15 km was extracted from an area where gneiss of the Proterozoic (AR2-PR1) occur.

[Western part of the Jarganant sheet area]

A circular structure having a diameter of 10 km was extracted from an area where alkali granites of the Permian (γ P2) occur, and a caldera-like concave was identified in its central part.

[Southeastern part of the Hutag sheet area]

A circular structure having a diameter of 15 km was extracted from an area where acid volcanic rocks of the Permian (Plv (1)) occur, and existence of a lineament

traversing in the E-W trend was identified in its central part. There is a conical depression at the center of the circular structure.

Figure II-2-8 shows a radar image around the circular structures described in western part of the Jarganant sheet area and southeastern part of the Hutag sheet area.

b. Western half of the target area

In this area, some ring structures were identified as detailed below. Among them, those extracted from the "Tosontsengel" and "Hatgal" images have a characteristic of being situated near the fracture zones or in their intersections.

[Southeastern part of the Dzurh sheet image]

An unclear ring structure having a diameter of 18 km was extracted from an area where granitic rocks of the Lower Proterozoic ($\gamma\ \delta$ PZ1) occur.

[Eastern part of the Tosontsenge sheet image]

A ring structure having a diameter of 10 km was extracted from an area where granitic rocks of the Lower Proterozoic and the Devonian ($\gamma\ \delta$ PZ1, γ D2) occur. This ring structure is situated in the south end of a fracture zone in the E-W direction.

[Southeastern part of the Chandmani sheet image]

Ring structures having diameters of several kilometers to 6 km are arranged from the EW to SE direction where granitic rocks of the Devonian (γ D2) occur.

[Eastern part of the Hatagal sheet image]

Unclear ring structures having diameters of 5 km or less are concentrated in an area where granitic rocks of the Lower Proterozoic($\gamma\ \delta$ PZ1) occur. This area corresponds to the intersection of fracture zones in the NE-SW and NW-SE directions, showing a complex structure.

[The south end of the Hatgat sheet image]

A double ring structure having a diameter of 8 km was extracted from an area where granitic rocks of the Devonian (γ D2) occur. This ring structure is located near the fracture zone in the NW-SE direction.

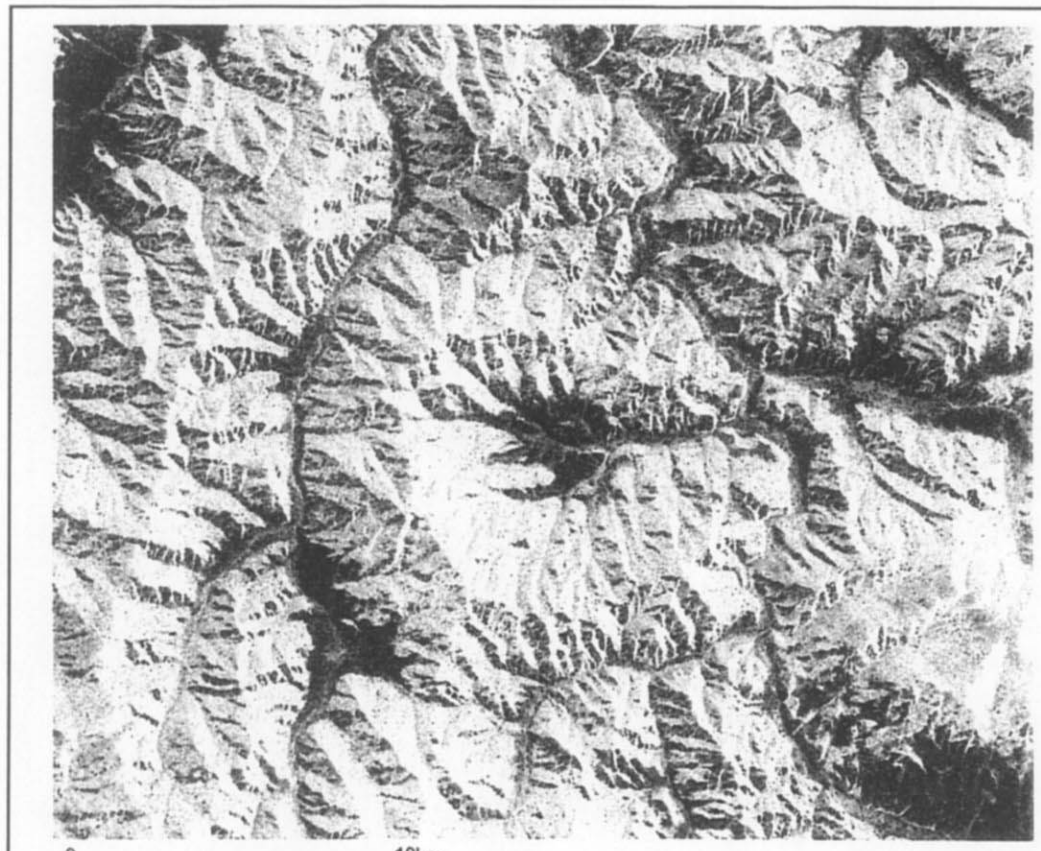

from Hutag image unit

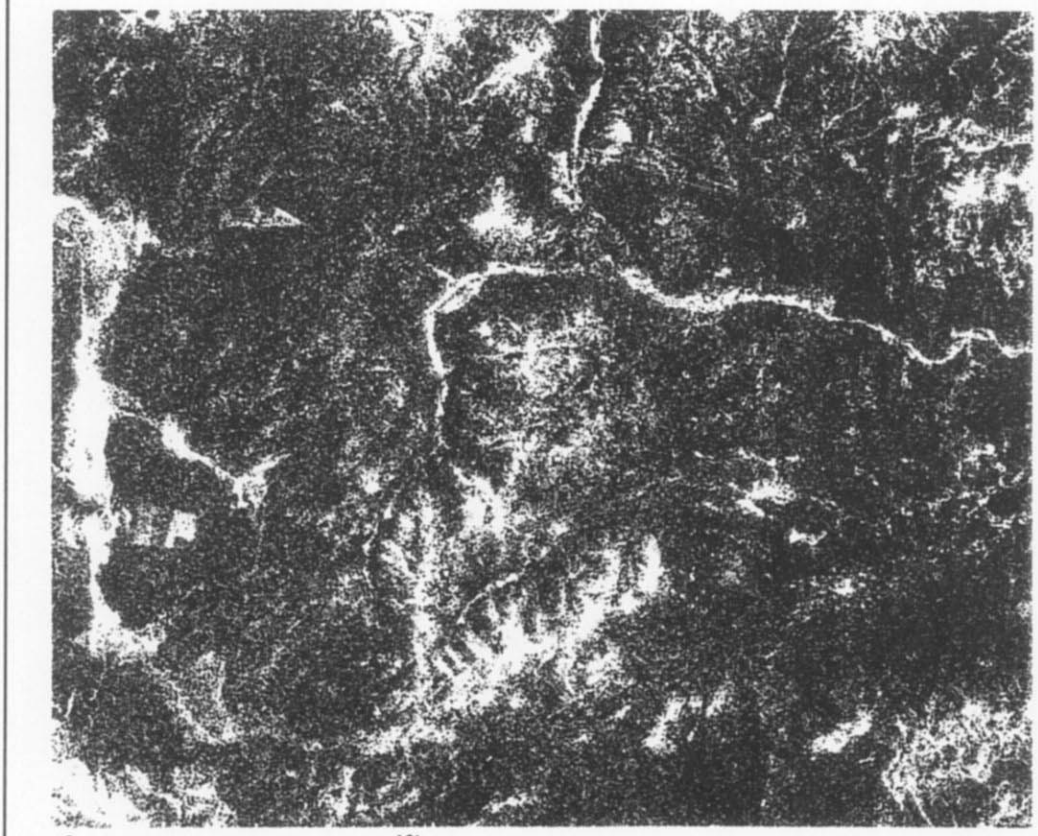

from Jarganant image unit

Fig. II-2-8 Circular feature extracted from JERS-1/SAR mosaic image (Hutag unit and Jarganant unit)

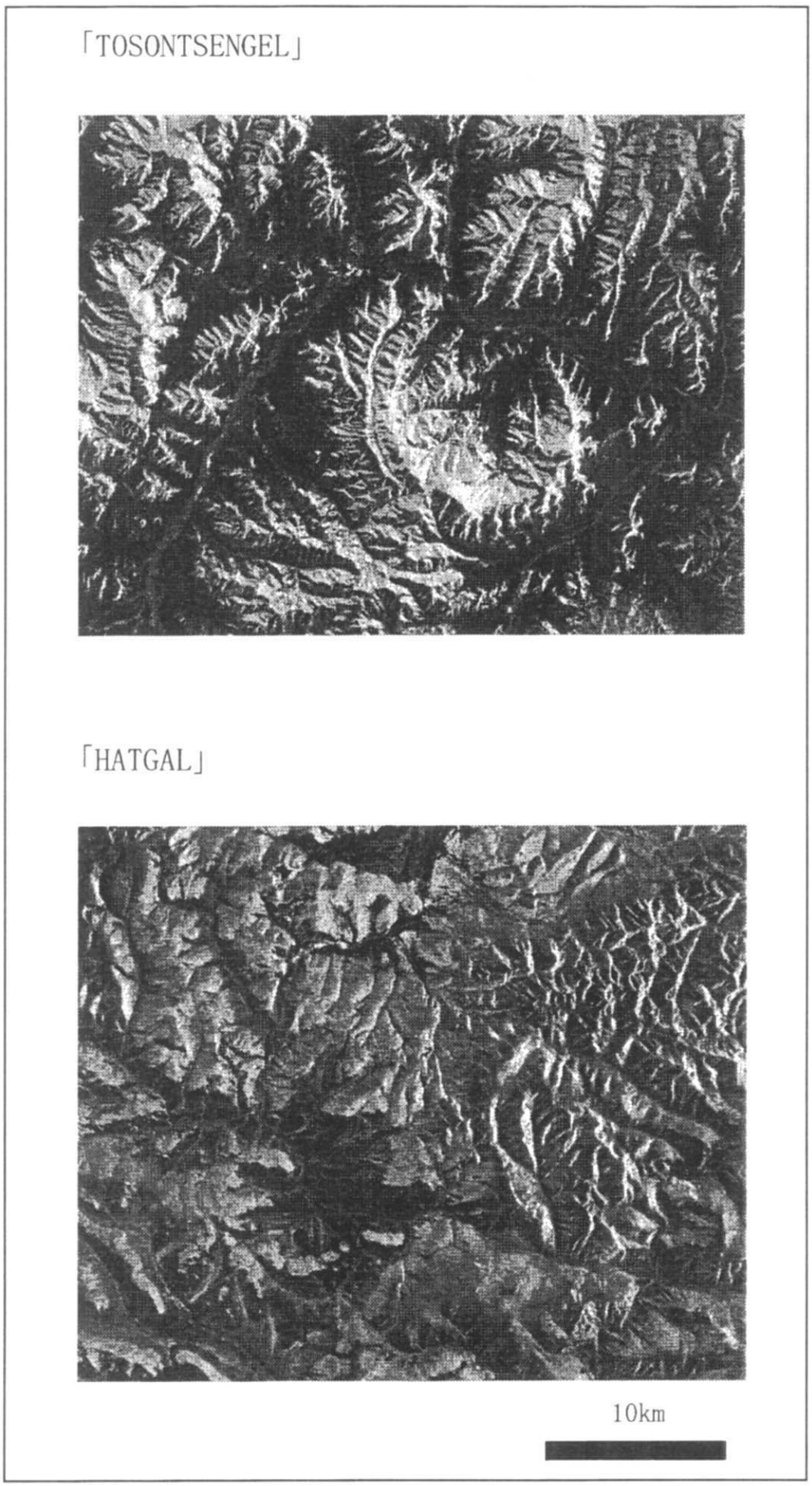

Fig. II-2-9 Circular feature extracted from JERS-1/SAR mosaic image (Tosontsengel unit and Hatgal unit)

Figure II-2-9 shows the radar images near the ring structures of b. and d. above.

2.2.4 Distribution of mineral occurrences

Figure II-2-10 shows distribution of mineral occurrences of gold, copper and molybdenum which is based on the existing data before this survey and plotted on the mosaic image. From this figure, distribution of mineral occurrences is summarized as follows:

(1) Gold

In eastern half of the target area, mineral occurrences of gold are located in the northeastern end, northern central part and the southeastern end of an area. In the northern central part of an area, every Au occurrence accompanies Cu mineralization.

In the western half of the area, mineral occurrences of gold are distributed in the northeastern central and southeastern parts. A lot of prospects are concentrated on the central part and their state consist of stockwork and quartz vein in many cases.

(2) Copper

In the eastern half of the target area mineral occurrences of copper are located not only in the entire district of the southern part, but also in the central part along having the NW-SE lineaments.

In the western half of the area, mineral occurrences of copper are widely distributed in the entire southern part as well as in the central-eastern part. Although the state in most cases consist of stockwork and quartz vein, prospects with small areas of altered zone are also identified.

(3) Molybdenum

In the eastern part of the target area, mineral occurrences of molybdenum are located accompanied with copper mineralization. Other occurrences were scattered all over the area.

In the western half of the area, a tendency is noted where mineral occurrences of molybdenum accompanied with gold and copper prospects are distributed from the central part to the central-eastern part. Many of the prospects which are widely distributed in the southern part are accompanied by mineral showing of copper. While their state consist of stockwork, quartz vein, fractures, skarn and greisen in the case of the prospects with molybdenum alone, they often form

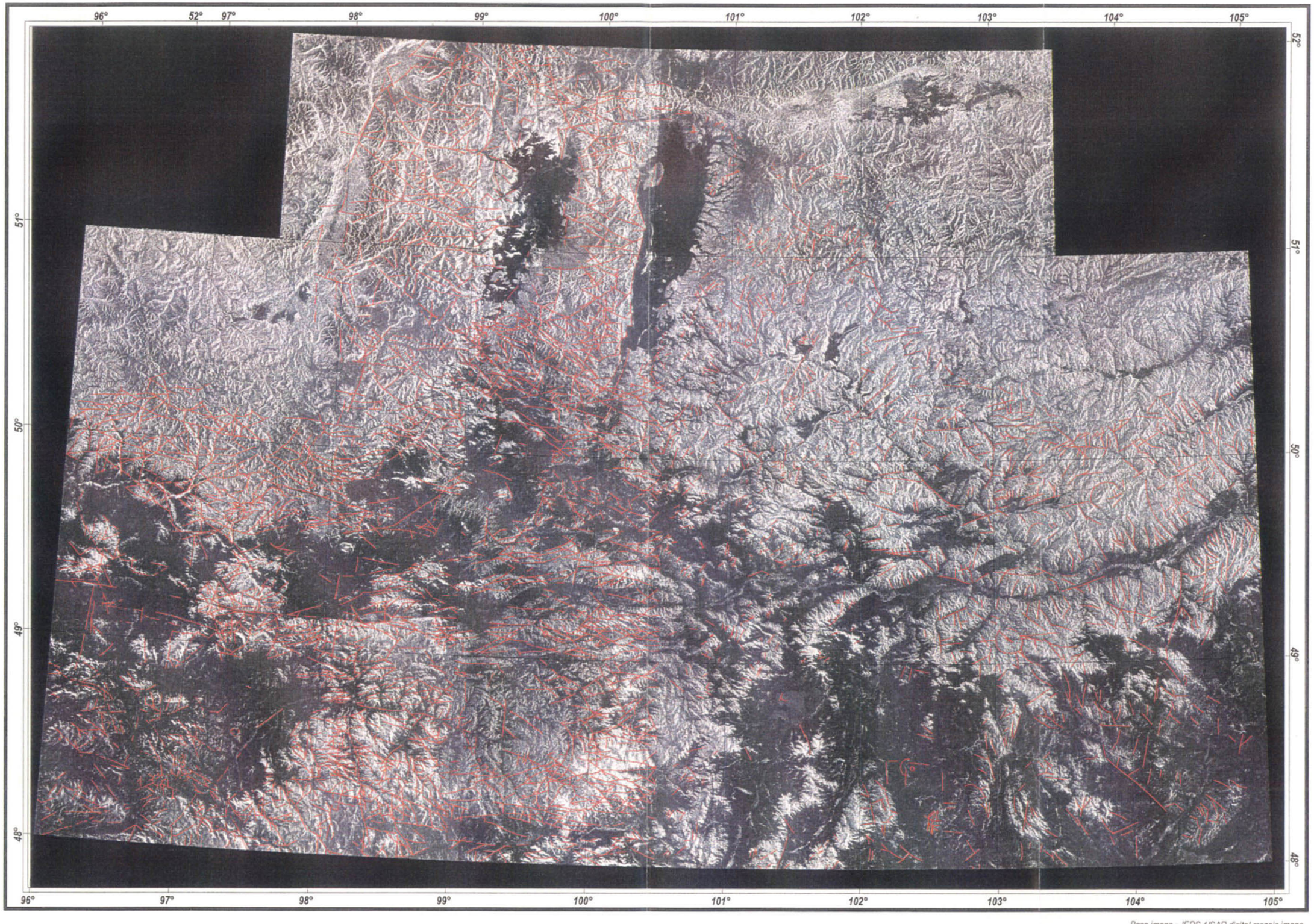

LEGEND

Structure

Lineament

50 0 50 100 km

Base image : JERS-1/SAR digital mozaic image

Fig. II-2-10 Liniament and circular feature extracted from JERS-1/SAR mosaic image

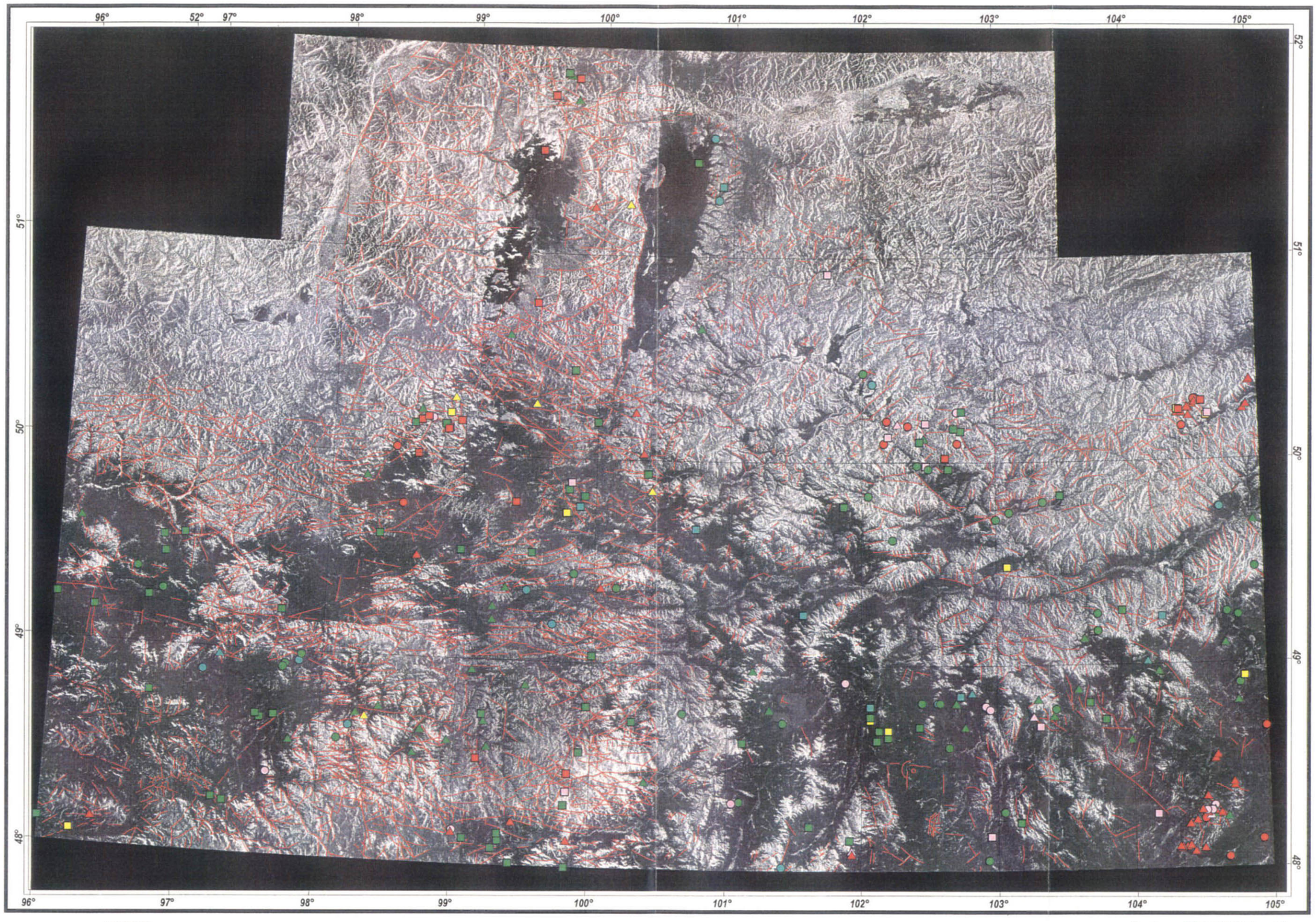

Fig. II-2-11 Liniament and circular feature extracted from JERS-1/SAR mosaic image with mineral occurrences on the image

altered zone when they are accompanied by copper.

2.2.5 Summary

Figure II-2-11 shows a mosaic image on which locations of lineaments, circular structures and mineral occurrences are indicated. Through comparison of the image analysis and interpretation with the existing mineral occurrences, the following six sites were extracted as targets to be surveyed.

(1) Eastern half of the target area

① Central to southern parts: Rashaant, Hutag and Bulgan image sheets
Mineral showing: Copper and gold
State: porphyry and mineral-vein types
Fracture: in the NW-SE direction
Others: The central part along the Egiyn River and the southeastern part of the Hutag image sheet where a ring structure was extracted are considered as promising.

②Southern part: western part of the Jarganant image sheet
Mineral Showing: Copper
State: Stockwork and quartz vein
Ring Structure: Existing on hilly grounds and a caldera-like concave land is identified. A small-scale rocks with altered zone may exist.

(2) Western half of the target area

① Central part: southern part of the Altraga image sheet
Mineral Showing: Gold, copper
State: Stockwork and quartz vein
Fracture: In the E-W/NE-SW directions, with high density
Others: Ring structures with diameters of several km to 6 km exists in the direction of northeast to

southeast. (granitic rocks of the Devonian)

② Central-Southern Part: northern part of the Tosontsengel image sheet
Mineral Showing: Gold, copper, molybdenum
State: Stockwork and quartz vein
Fracture: Fractures in the E-W direction or those derived from such fractures
Others: Existence of a ring structure with a diameter of 10 km (Granitic rocks of the Lower Proterozoic and Devonian)

③ South-eastern Part: center and western part of the Dzurh image sheet
Mineral Showing: Copper
State: Stockwork and quartz vein
Fracture: Intersection of fracture zones in the N-S and NE-SW directions
Others: The fracture zone in the N-S direction consists of the fractures in the NW-SE/NE-SW directions

④ Central-Northern Part: western part of the Hatgal image
Mineral Showing: Gold and copper
State: Fractures, skarn, greisen, stockwork and quartz veins
Fracture: Intersection of fracture zones in the NE-SW and NW-SE directions
Others: Unclear ring structures with diameters of 5 km or less are concentrated (Granitic rocks of the Lower Proterozoic.

2.3 Processing of the LANDSAT TM image

2.3.1 Introduction

Spectrum analysis of LANDSAT TM data was conducted to study the possibility of extracting alteration zones in the Erdenet deposit and its peripheral area. The target area is rectangular from 102°20' E to 104°40' E in the east and west direction and from 48°30' N to 49°20' N in the north and south direction and includes the Erdenet mine on the east of the area.

2.3.2 Satellite data

The following two scenes of TM data were used in the analysis.

Table II-2-4 LANDSAT TM data used in the analysis

Path	Row	Acquisition date	Remarks
P134	R26	1989/09/27	Central to West of the area: Erdenet mine is not included.
P133	R26	1989/06/09	Central to East of the area: Erdenet mine is included.

(1) False color image

For band combination, (B), (G), (R) were allocated to BN1, BN4, BN5, respectively to extract the general characteristic of the entire target area. Also, a digital conjugating of image data located on the east and west was conducted so that the peripheral area of the Erdenet deposit can be read at a glance. The Lambert regular cone projection method was adopted. For a DN value, a method of incorporating image data (P133-R26) on the east was used with image data (P134-R26) on the west being a reference.

The output image data is shown in Figure II-2-12, 13, and 14.

(2) Ratio composite image

Ratio composite image was applied as a simple method of knowing signs pointing to the possibility of the extraction of alteration minerals, and the output image was prepared. For band combination of rationing since the LANDSAT TM data has two bands in the shorter wavelength infrared range, band 5/7, 3/1, and 5/4 were allocated to B, G, and R, respectively to output a color ratio composite image. The features of each ratio composite is as shown below:

B: 5/7: Extraction of clay minerals. A red portion may be an alteration zone.

G: 3/1: Extraction of iron minerals.

R: 5/4: Extraction of clay and iron minerals. Apparent reduction of affection to vegetation.

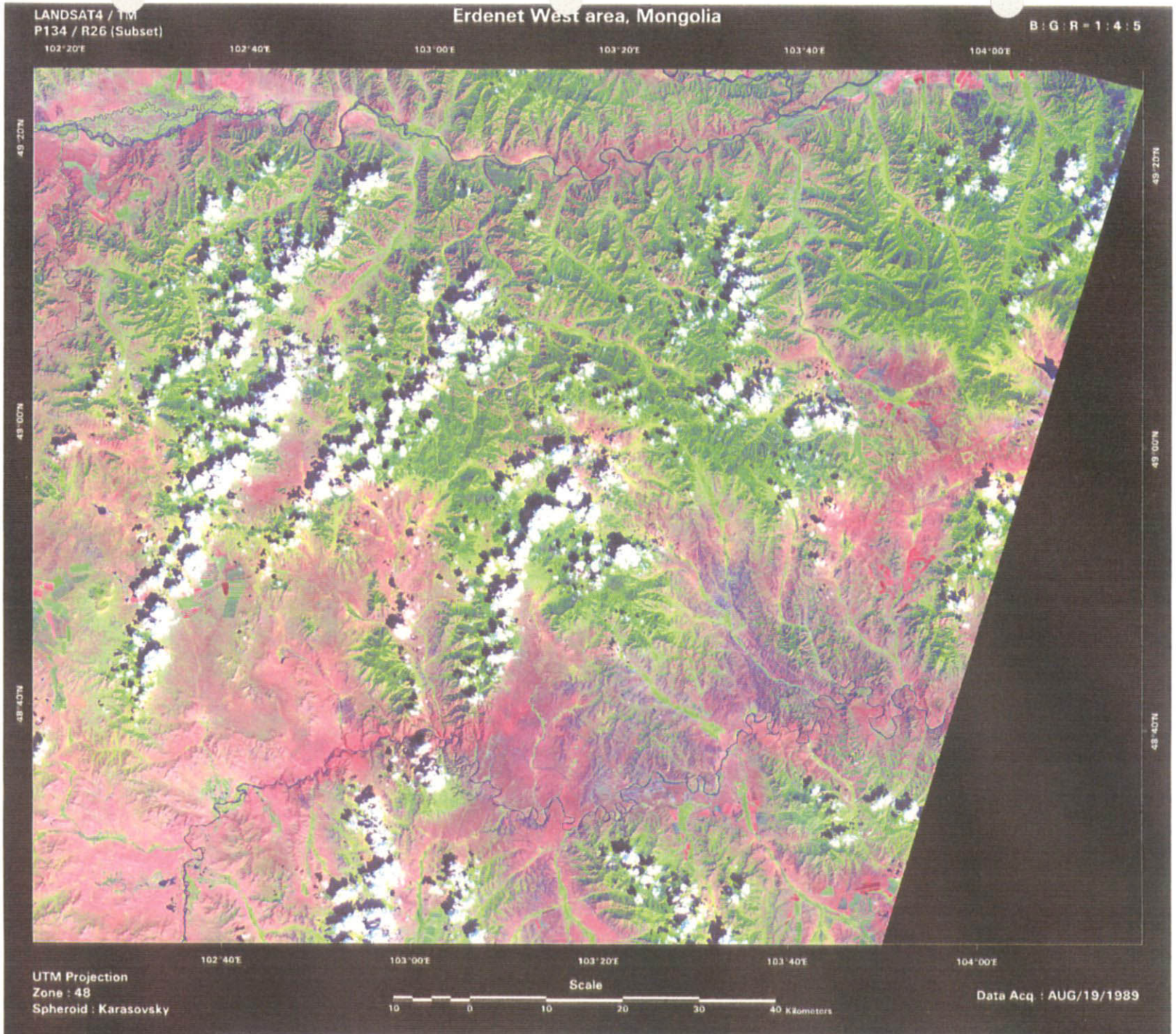

Fig. II-2-12 LANDSAT TM false color image of the Erdenet West area (western part)

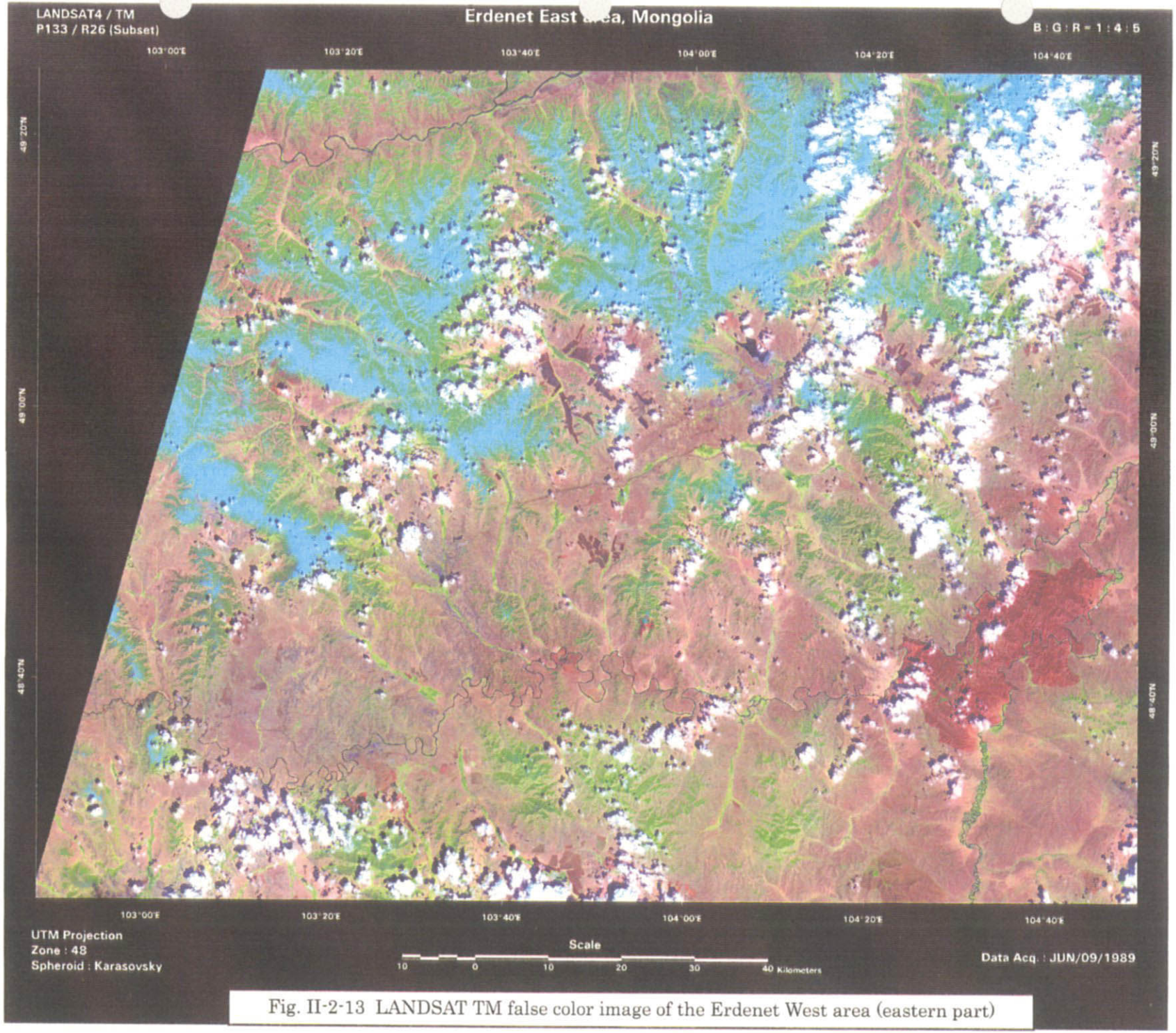

Fig. II-2-13 LANDSAT TM false color image of the Erdenet West area (eastern part)

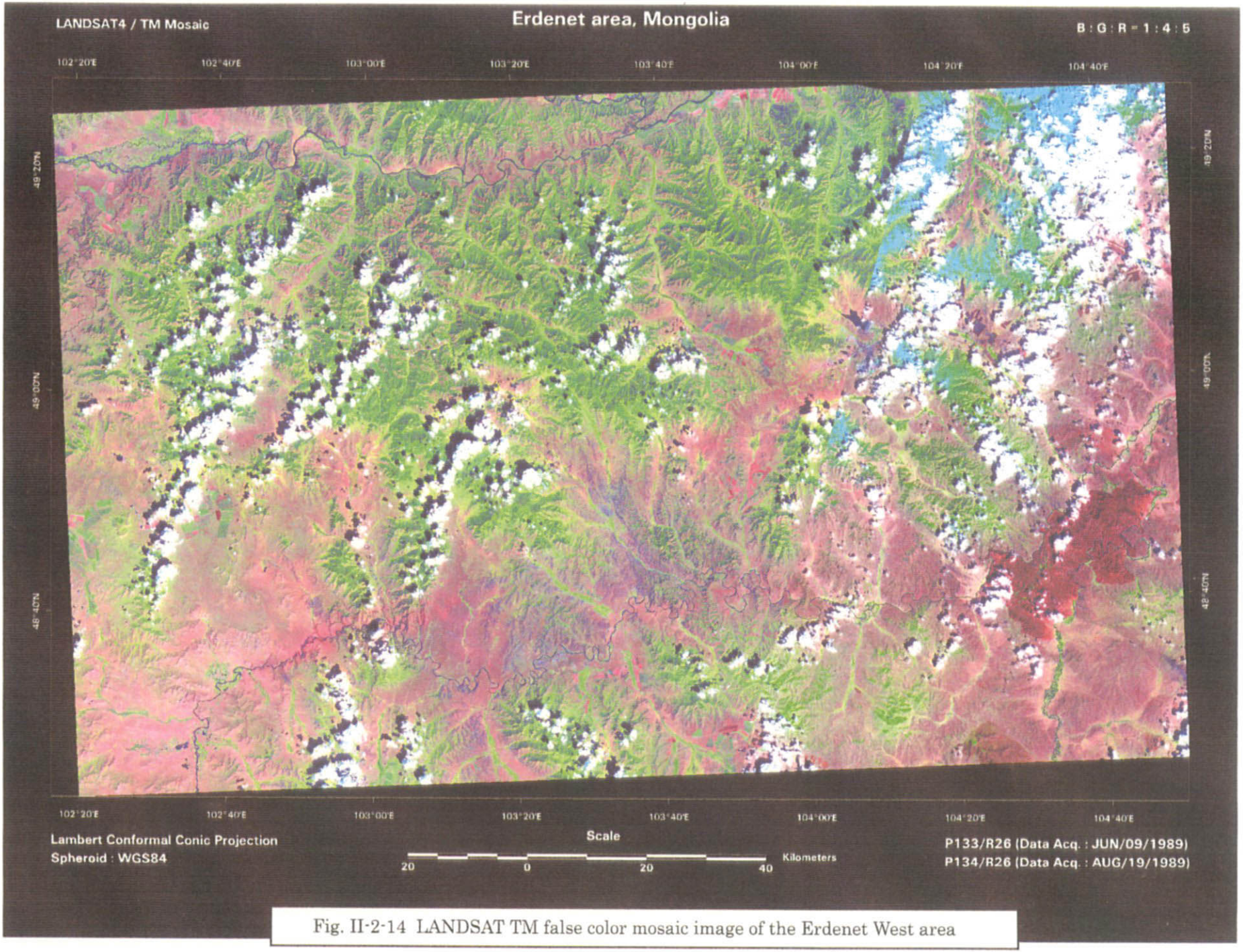

Fig. II-2-14 LANDSAT TM false color mosaic image of the Erdenet West area

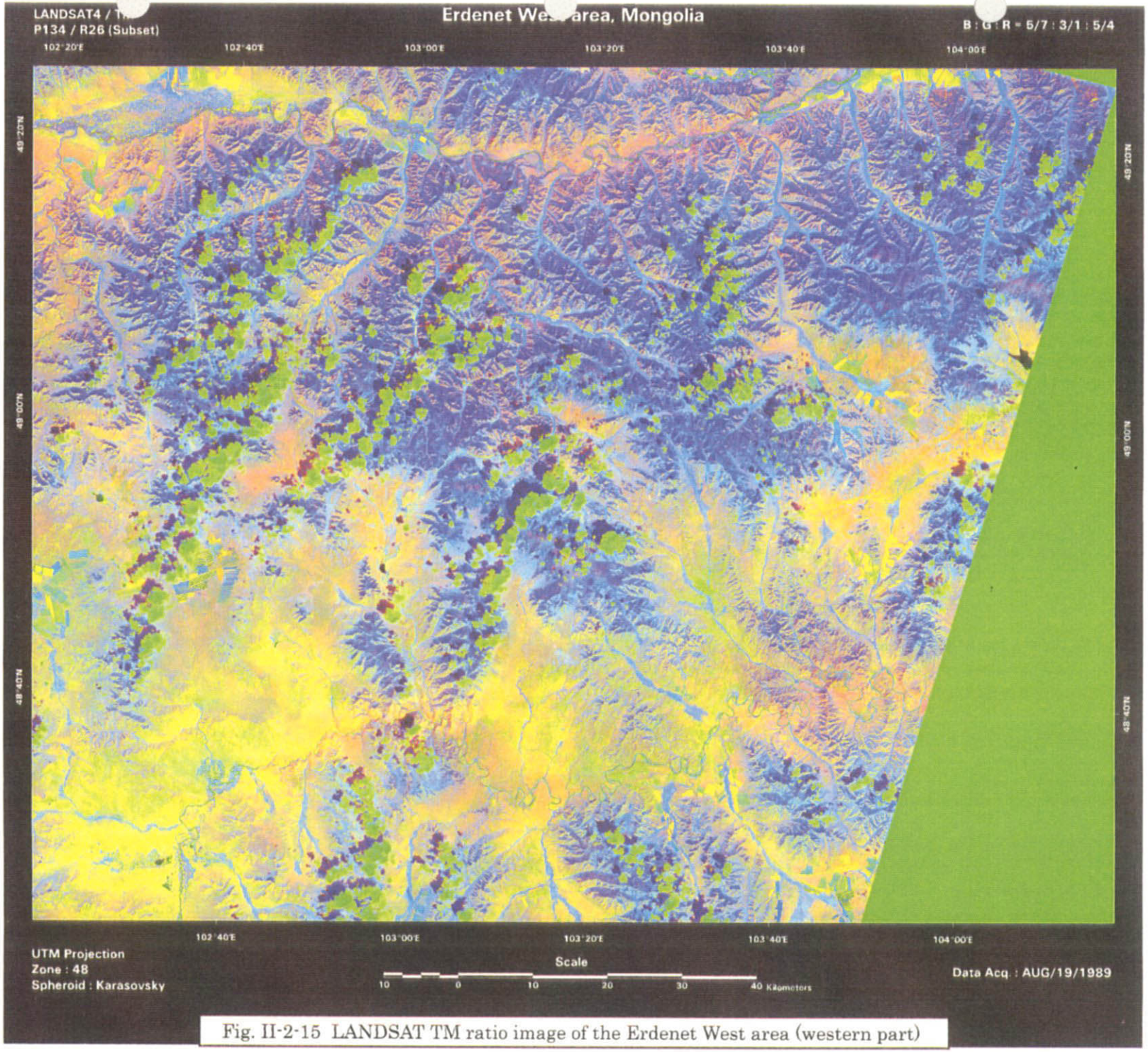

Fig. II-2-15 LANDSAT TM ratio image of the Erdenet West area (western part)

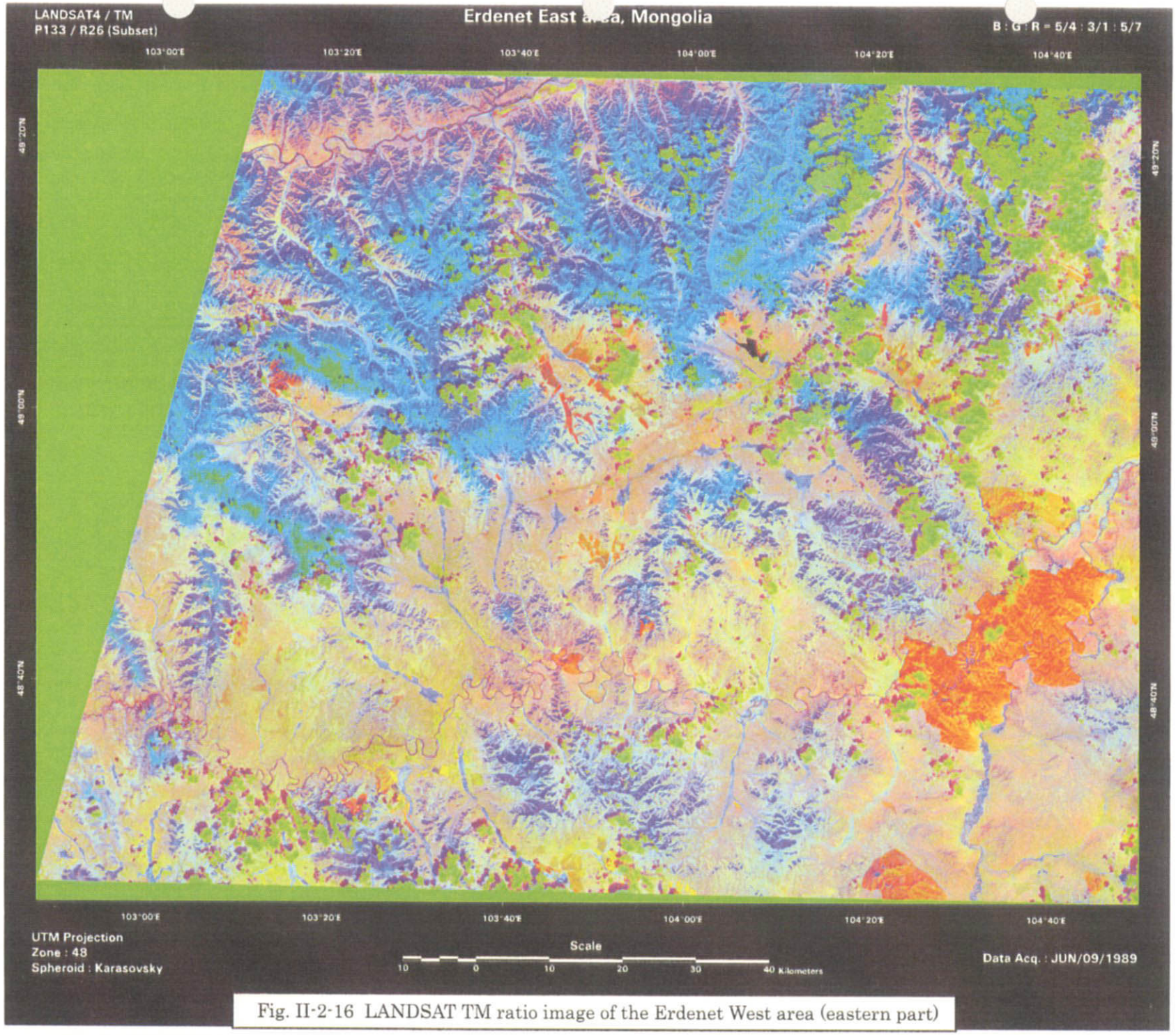

Fig. II-2-16 LANDSAT TM ratio image of the Erdenet West area (eastern part)

The output image data is shown in Figure II-2-15 and 16.

2.3.3 Data processing

The classification was conducted by using the image characteristics of known deposits and alteration zones. The classification refers to the processing of classifying pixels into specified individual classes and categories based on image data file values. The method used for this survey is as shown below:

(1) Definition of signature: A bank of tailing dam in the northern part of the Erdenet mine and the Tsagaan chuluut alteration zone were selected as a standard to define them as a characteristic amount on the image.

Note) In the beginning, an open pit of the Erdenet mine was scheduled to be selected as a standard. Since the obtained image showed that the pit was covered with cloud, a bank of tailing dam composed of detritus dug out of this pit was selected as a substitute.

(2) Evaluation of signature: The separation rate between Contingency Matrix and signature is an important evaluation item. The former is classified within the range of a selected standard based on its signature, and weights are assigned to the statistic so that as many pixels as possible can be selected. The latter was allowed to select a classification algorithm, and the maximum likelihood method was used for this survey to evaluate its separation rate.

(3) Execution of classification: There are two decision rules for the classification: non-parametric and parametric. In this survey, the most likelihood method was executed for a parametric signature.

(4) Evaluation of classification: After the classification was executed, the classification was evaluated based on the superimposition of the classification, the setting of a threshold, and the recording of a class, and the final image was output.

The color tone of the final image is as shown below:

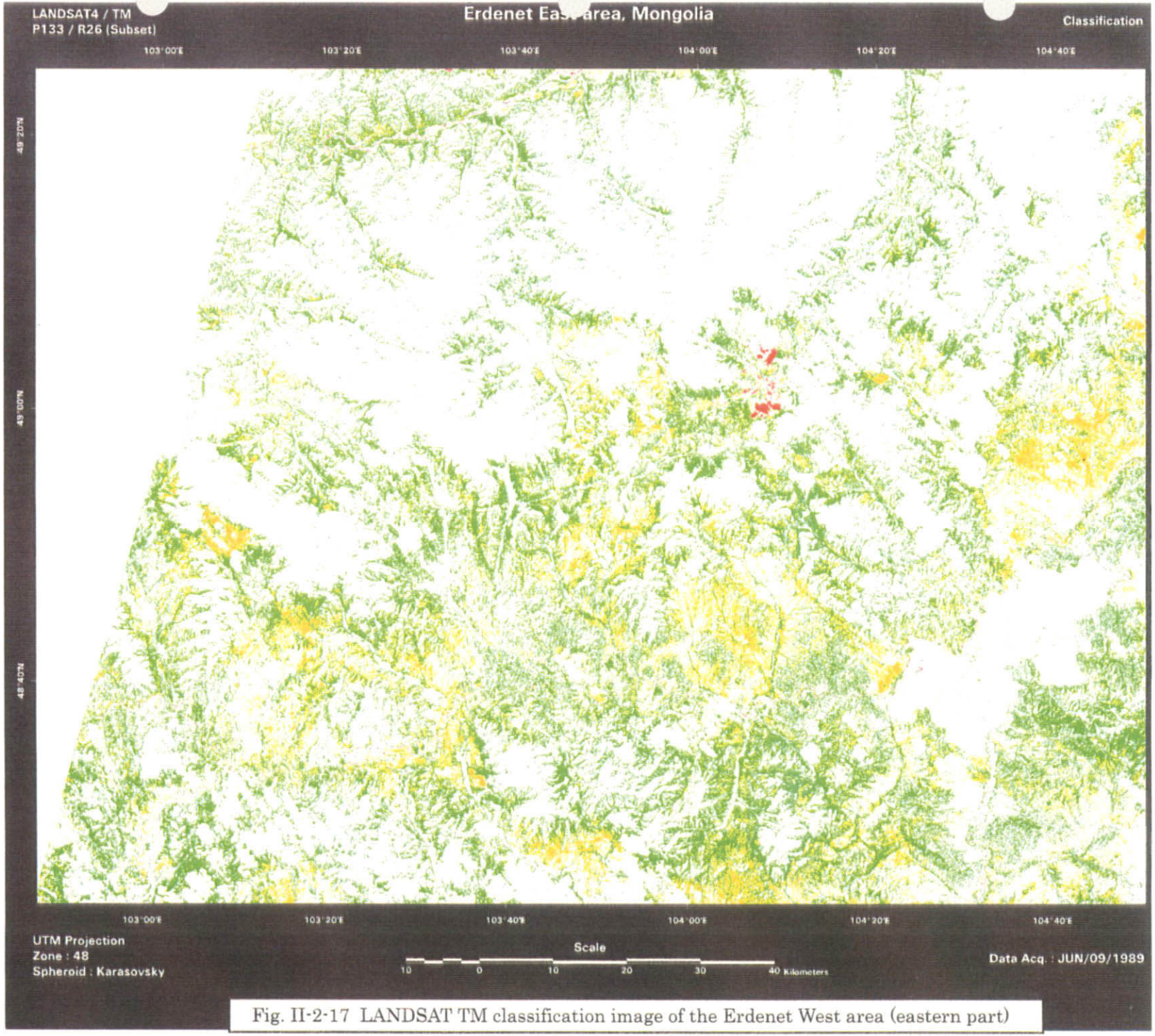

Fig. II-2-17 LANDSAT TM classification image of the Erdenet West area (eastern part)

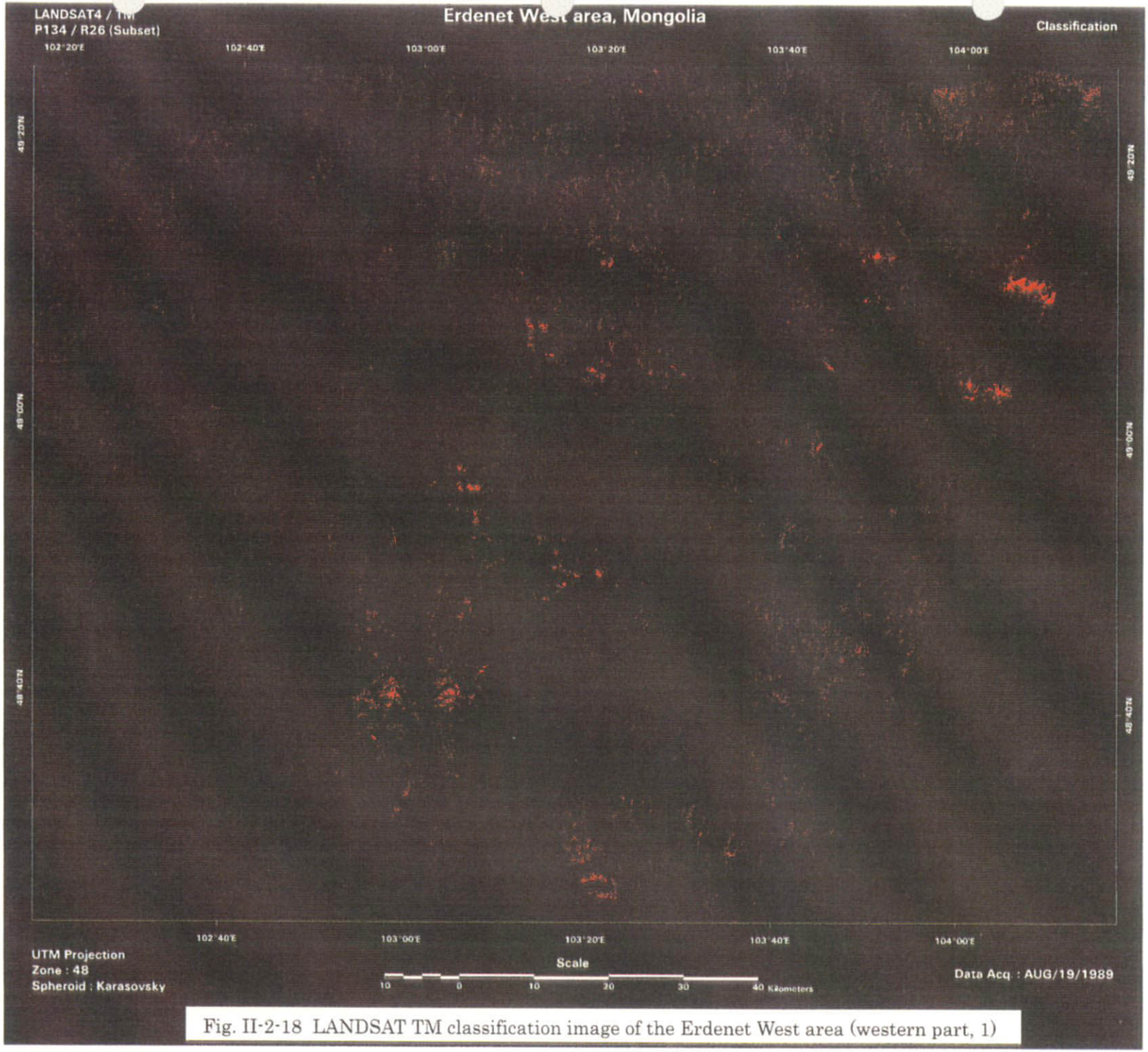

Fig. II-2-18 LANDSAT TM classification image of the Erdenet West area (western part, 1)

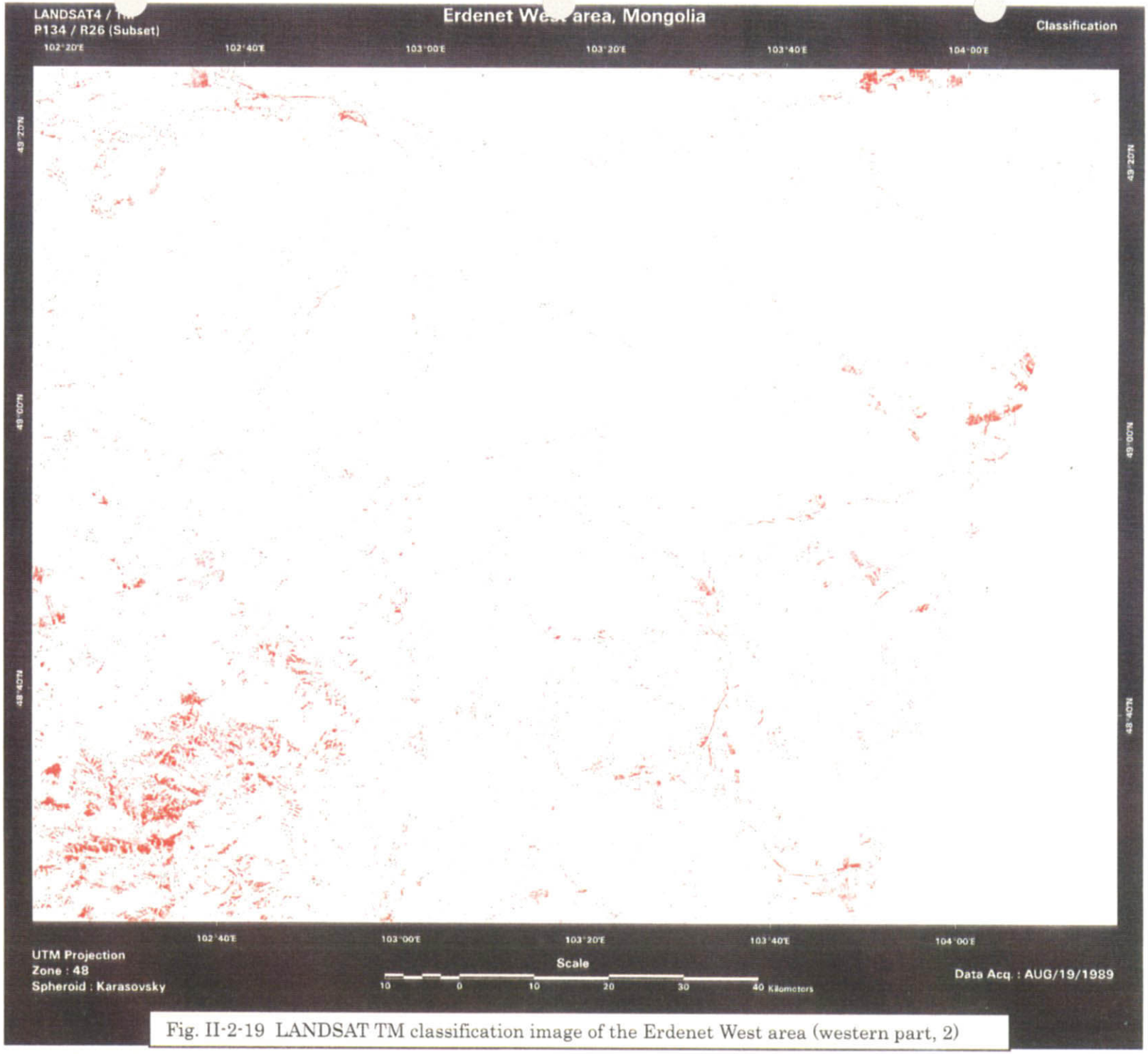

Fig. II-2-19 LANDSAT TM classification image of the Erdenet West area (western part, 2)

Table II-2-5 Data on the image of the eastern part of the Central north area (P133-R26)

Model area	Color tone of the image
Open pit of the Erdenet mine	red
Trench at the south-eastern area	orange
Alteration zone closed to the open pit of the Erdenet mine	green

Table II-2-6 Data on the image of the western part of the Central north (P134-R26)

Model area	Color tone of the image
Bank of the dam (corresponding to the Open pit of the Erdenet mine)	red
Known alteration zones (North of the area)	red

The output image data is shown in Figure. II-2-17, 18, 19.

2.3.4 Summary

(1) East side of the district (Figure II-2-17)

Red: An anomaly with a diameter of several kilometers was extracted about 7 km north of the open pit of the Erdenet mine.

Orange: Compared to the false color image, it seems to have been extracted universally in a portion of a color tone of an exposed rock area.

Green: Compared to the false color image, it was extracted universally in an exposed rock area, particularly in correspondence with the topography. This may be attributable to the fact that reflection spectra on the earth's surface in a specified direction were selectively extracted.

(2) West side of the district 1 (Erdenet West area: Figure II-2-18)

Red: It is slightly difficult to discern the character because of the dark background. Compared to the false color image, it seems to have been extracted in correspondence with an elevation of the exposed rock area.

(3) West side of the district 2 (Erdenet West area: Figure II-2-19)

Red: Compared to the false color image, it was extracted in correspondence with the topography in the southwestern part and in correspondence with man-made structures such as roads and fields in another part.

Judging from the results above, it was concluded that the LANDSAT TM image currently processed and prepared could not serve as an index for extracting a hydrothermal alteration zone and the image was excluded from the Grand Truth reference data. This area, particularly, the peripheral area of the Erdenet mine has well-developed soil on the whole and rises and falls in gentle arcs. It is thought that a clear alteration area could not be extracted because the majority of the area is covered thickly with vegetation.

Nevertheless, small-scale exposed rock exists in such an area. In reality, a large amount of exposed rock was discovered in the process of the geologic survey of the earth's surface and some exposed rock was sampled. In such an area covered with vegetation, the extraction of an exposed rock area (or a low vegetation rate area) prior to a geologic survey by using an optical sensor image such as the LANDSAT TM will greatly contribute to the planning of a efficient geologic survey route.